AD-A067 948 BALL BROS RESEARCH CORP BOULDER COLO AEROSPACE DIV F/G 9/5
MICROSTRIP MILLIMETER WAVE ANTENNA STUDY.(U)
APR 79 M A WEISS, R B CASSELL DAAB07-77-C-0158
UNCLASSIFIED F78-16 CORADCOM-77-0158-F NL

| OF |
AD
A067948

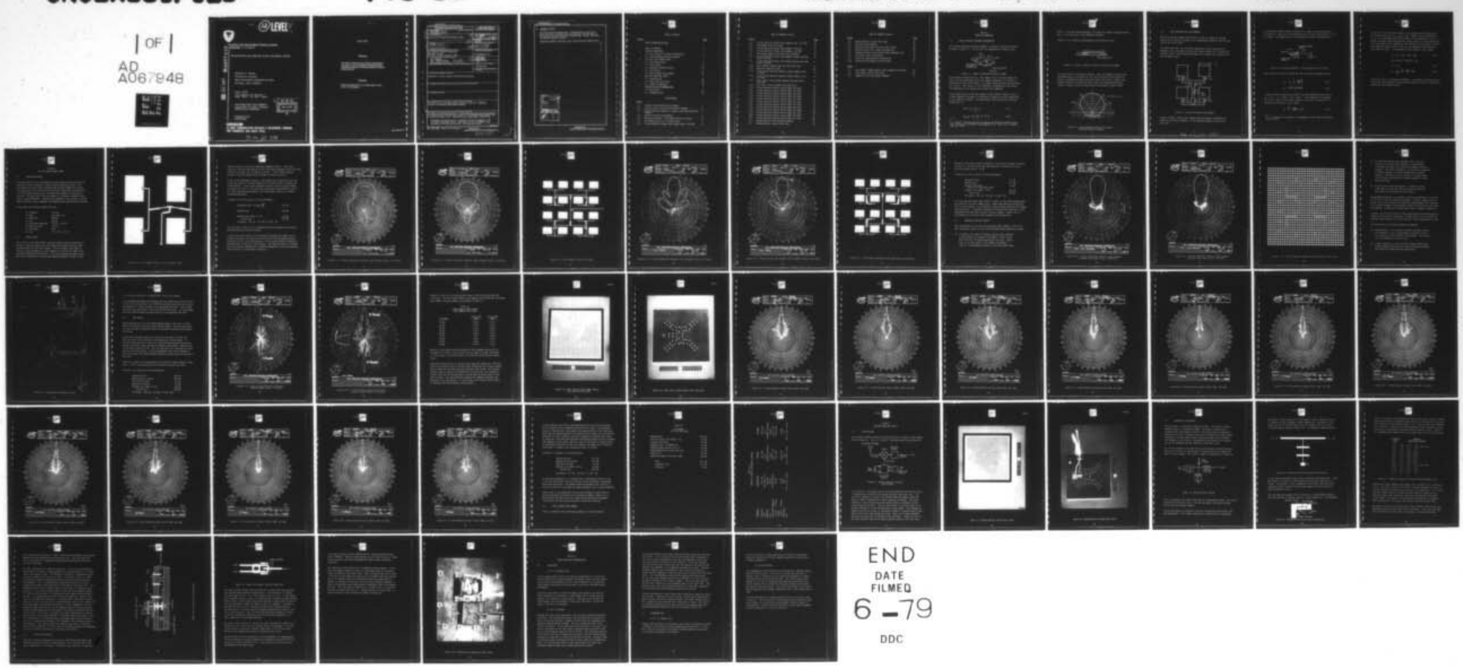

END
DATE
FILMED
6 - 79
DDC

— (12) LEVEL II

SC

RESEARCH AND DEVELOPMENT TECHNICAL REPORT
CORADCOM- 77-0158-F

AD A067948

DDC FILE COPY

MICROSTRIP MILLIMETER WAVE ANTENNA STUDY

Michael A. Weiss
Richard B. Cassell
Ball Aerospace Systems Division
Boulder, Colo. 80306

April 1979
Final Report for Period 1
Aug. 1977 - 31 Oct. 1978

DISTRIBUTION STATEMENT
Approved for public release;
distribution unlimited.

Prepared for:
CENCOMS

CORADCOM
US ARMY COMMUNICATION RESEARCH & DEVELOPMENT COMMAND
FORT MONMOUTH, NEW JERSEY 07703

79 04 25 098

NOTICES

Disclaimers

The citation of trade names and names of manufacturers in this report is not to be construed as official Government indorsement or approval of commercial products or services referenced herein.

Disposition

Destroy this report when it is no longer needed. Do not return it to the originator.

UNCLASSIFIED

SECURITY CLASSIFICATION OF THIS PAGE (When Data Entered)

19 REPORT DOCUMENTATION PAGE		READ INSTRUCTIONS BEFORE COMPLETING FORM
1. REPORT NUMBER 18 CORADCOM-77-0158-F	2. GOVT ACCESSION NO.	3. RECIPIENT'S CATALOG NUMBER
4. TITLE (and Subtitle) 6 Microstrip Millimeter Wave Antenna Study.		5. TYPE OF REPORT & PERIOD COVERED 9 Final Report. 1 Aug 1977 - 31 Oct 1978,
		6. PERFORMING ORG. REPORT NUMBER 14 F78-16
7. AUTHOR(s) 10 Michael A./Weiss Richard B./Cassell		8. CONTRACT OR GRANT NUMBER(s) 15 DAAB07-77-C-0158
9. PERFORMING ORGANIZATION NAME AND ADDRESS Ball Brothers Research Corporation Aerospace Division/ Box 1062, Boulder, Colorado 80306		10. PROGRAM ELEMENT, PROJECT, TASK AREA & WORK UNIT NUMBERS 611102-H48-H2-11-01
11. CONTROLLING OFFICE NAME AND ADDRESS Cdr, CORADCOM ATTN: DRDCO-COM-RM-4 Fort Monmouth, NJ 07703	12 60p.	12. REPORT DATE 11 April 1979
		13. NUMBER OF PAGES 55
14. MONITORING AGENCY NAME & ADDRESS (if different from Controlling Office)		15. SECURITY CLASS. (of this report) UNCLASSIFIED
		15a. DECLASSIFICATION/DOWNGRADING SCHEDULE

16. DISTRIBUTION STATEMENT (of this Report)

Approved for public release; distribution unlimited.

17. DISTRIBUTION STATEMENT (of the abstract entered in Block 20, if different from Report)

18. SUPPLEMENTARY NOTES

19. KEY WORDS (Continue on reverse side if necessary and identify by block number)

Microstrip Array, Millimeter Waves, Receiver Front End, Integrated Microstrip Millimeter Wave Receive Antenna

20. ABSTRACT (Continue on reverse side if necessary and identify by block number)

The study was conducted primarily to investigate the feasibility and potential of integrating the front-end mixer circuit of a millimeter wave receiver into a microstrip antenna array. Development was concentrated in three areas:

Investigate the practicality of conformal microstrip antennas in the millimeter wavelength region. Specifically a 32 X 32 element array operating at 38.4 GHz was designed, fabricated and tested.

(Cont'd)

DD FORM 1 JAN 73 1473 EDITION OF 1 NOV 65 IS OBSOLETE

UNCLASSIFIED

SECURITY CLASSIFICATION OF THIS PAGE (When Data Entered)

409 767

20. ABSTRACT (Cont'd)

Investigate possible designs for a front-end mixer circuit (i.e., local oscillator and mixer) which are compatible with the goal of incorporation into the microstrip antenna array. Design, fabricate, and analyze candidate circuits.

Integrate candidate front-end circuit into microstrip antenna array.

ACCESSION for		
NTIS	White Section	☑
DDC	Buff Section	☐
UNANNOUNCED		☐
JUSTIFICATION		
BY		
DISTRIBUTION/AVAILABILITY CODES		
Dist.	AVAIL. and/or SPECIAL	
A		

TABLE OF CONTENTS

ILLUSTRATIONS

TABLE OF CONTENTS (Cont'd)

TABLE OF CONTENTS (Cont'd)

Section 1
THEORY OF MICROSTRIP

1.1 BASIC MICROSTRIP ANTENNA CONFIGURATION

The linearly polarized microstrip element is basically a two-slot radiator[1] as shown in Figure 1-1. The two slots are separated by a length of very

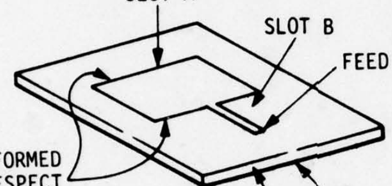

Figure 1-1 Linearly Polarized Microstrip Element

low impedance transmission line. The length of this line can be made just short of a half wavelength so that the complex admittance G_s of Slot A is transformed to G_s^* at Slot B where it is added in parallel with the admittance G_s of Slot B. The result is a real admittance corresponding to the radiation admittance of the antenna plus a small loss component.

Losses depend mostly on the loss tangent of the dielectric material and to a lesser degree on thickness of the dielectric material and the conductivity of the conducting surfaces. The dimensions of the cavity may be expressed analytically as:

$$L_{slot} \approx \frac{\lambda}{2} \left(\frac{1}{\sqrt{\varepsilon_r}}\right) \quad (1\text{-}1)$$

$$L_{cavity} \approx \frac{\lambda}{2} \left(\frac{K}{\sqrt{\varepsilon_r}}\right), \text{ for } K<1 \quad (1\text{-}2)$$

1 R. E. Munson, "Conformal Microstrip Antennas and Microstrip Phased Arrays," IEEE Transactions on Antennas and Propagation, Vol. AP-22, No. 1, January 1974, pp. 74-78.

where λ is the free space wavelength, K accounts for radiator edge capacitance, and ε_r is the real part of the dielectric constant.

Figure 1-2 is a sectional representation of the electric field

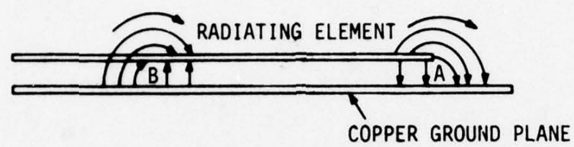

Figure 1-2 Electric Fields in Vicinity of Microstrip Element

in the vicinity of a microstrip radiator. Since the element is about a half wavelength long in the dielectric, the field at one end of the microstrip cavity is reversed from that at the other end of the cavity. However, the radiated fields are in phase and tend to add in the broadside direction. Figure 1-3 shows a typical E-plane pattern attributable to these fields.

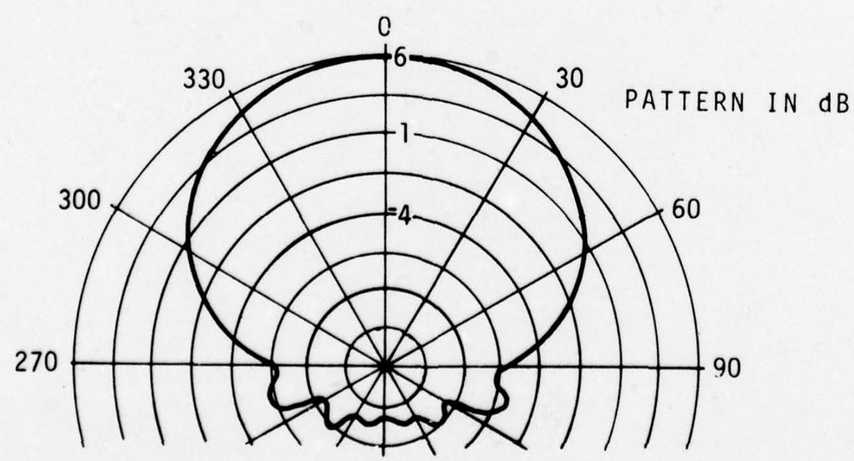

Figure 1-3 E-Plane Radiation Pattern of Linearly Polarized Microstrip Element

1.2 INPUT IMPEDANCE AND FEED NETWORKS

Microstrip antenna elements may be fed by a feed line etched on the same surface as the radiating element or by a feedthrough connection from the rear side of the circuit board.

For etched feed lines the line width required for a given characteristic impedance can be calculated using the well-known formulas for a narrow strip conductor above a conducting ground plane or by reference to an empirically-derived design curve.

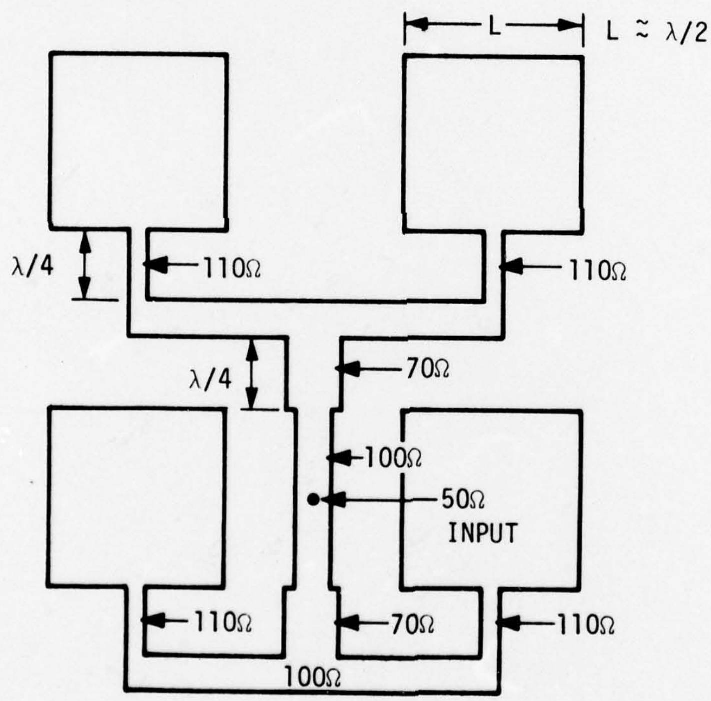

Figure 1-4 Typical Microstrip Feed Network

Figure 1-4 shows a typical feed network using quarterwave transformers to transform the driving impedance of the radiating element to that of the input port.

The microstrip radiator shown in Figure 1-4 is shown in cross-section view in Figure 1-5. Gap A is an infinitesimal slot (in 0.010" microstrip $a/\lambda \approx 0.03$ at 35 GHz). The admittance of a slot radiator is given in Harrington[3] for

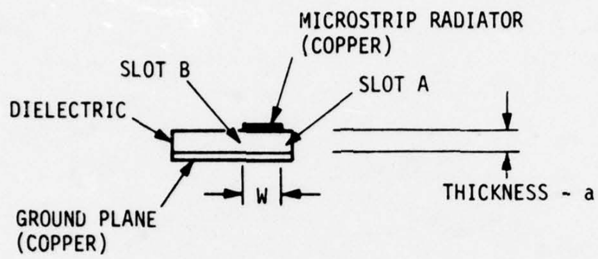

Figure 1-5 Microstrip Radiator - Cross Section View in L-Plane

small ka($a/\lambda<0.1$) which is always the case in microstrip antenna practice.

$$G_a \approx \frac{\pi}{\lambda\eta}\left[1 - \frac{(ka)^2}{24}\right] \quad (1\text{-}3)$$

$$B_a \approx \frac{3.134 - 2\log ka}{\lambda\eta} \quad (1\text{-}4)$$

In most microstrip applications $ka/24<<1$ and the conductance simplifies to $G_a = \pi/\lambda\eta = 1/(\lambda\cdot120\Omega)$ or $R_a' = 120\lambda\Omega$. The conductance is expressed in per unit length so that the resistance of the Slot A in Figure 1-5 is obtained by dividing R_a' by the length

$$R_a = \frac{R_a'}{L} = \frac{120\lambda\Omega}{\lambda/2} = 240\Omega \quad (1\text{-}5)$$

[3] R. F. Harrington, Time Harmonic Electromagnetic Fields, New York, McGraw Hill, p. 276.

In the case of the microstrip radiator, the conductance and susceptance of Slots A and B are equal ($G_a = G_B$, $B_a = B_B$). However, when the admittance of Slot B is transformed across the radiator to the feedpoint of Slot A, it becomes conjugate complex provided the radiator width is chosen appropriately. Since the characteristic impedance of the transmission line formed by radiating element and ground plane is very low, the appropriate width deviates only slightly from $\frac{\lambda}{2}$. The admittance at the feedpoint then becomes:

$$Y_F = (G_a + iB_a) + (G_B - iB_B) \qquad (1\text{-}6)$$

and since $B_a = B_b$ and $G_a = G_B$

$$Y_F = 2\,G_a \qquad (1\text{-}7)$$

$$R_F = \frac{1}{2G_a} = \frac{R_a}{2} = \frac{240}{2} = 120\Omega \qquad (1\text{-}8)$$

In practice, this is the measured impedance. This theory is accurate in predicting the input impedance for many designs each with different frequencies, thicknesses, and radiator widths.

Section 2
38.4 GHz 32x32 ELEMENT ARRAY

2.1 ARRAY DESIGN GOALS

The overall goal of this investigation was to establish the practicality of conformal microstrip antennas in the millimeter wavelength region. The investigation utilized results obtained under Contract DAAB07-76-C-0110 as a starting point, and continued with the design, development and fabrication of a 32x32 element antenna array, including feed system, for operation at 38.4 GHz. The input port of the feed system is a standard rectangular waveguide of Type WR-28(RG-96). Antenna array parameters, such as gain, side-lobe level, efficiency, input impedance, and bandwidth were measured and calculated.

Design goals for the 32x32 element array are:

• Frequency	38.4 GHz
• VSWR	Less than 1.5:1
• Bandwidth	200 MHz
• Gain	≥30 dB
• Half-Power Beamwidth	$(2^{o}-4^{o}) \times (2^{o}-4^{o})$
• Side-Lobe Level	<-20 dB
• Efficiency	>50%
• Size	5.5" x 5.5" x 0.25"

2.2 ARRAY DESIGN

Initial work on the 32x32 element array was directed toward optimization of the basic radiating element and a 2x2 element array which was used as the "building block" for the final antenna. This 2x2 element array shown in Figure 2-1, was developed at a scale frequency of 3.07 GHz on 0.063" thickness Duroid 5880 substrate material. This scale frequency was chosen using the ratio of thickness of the available substrate material (0.063") to the

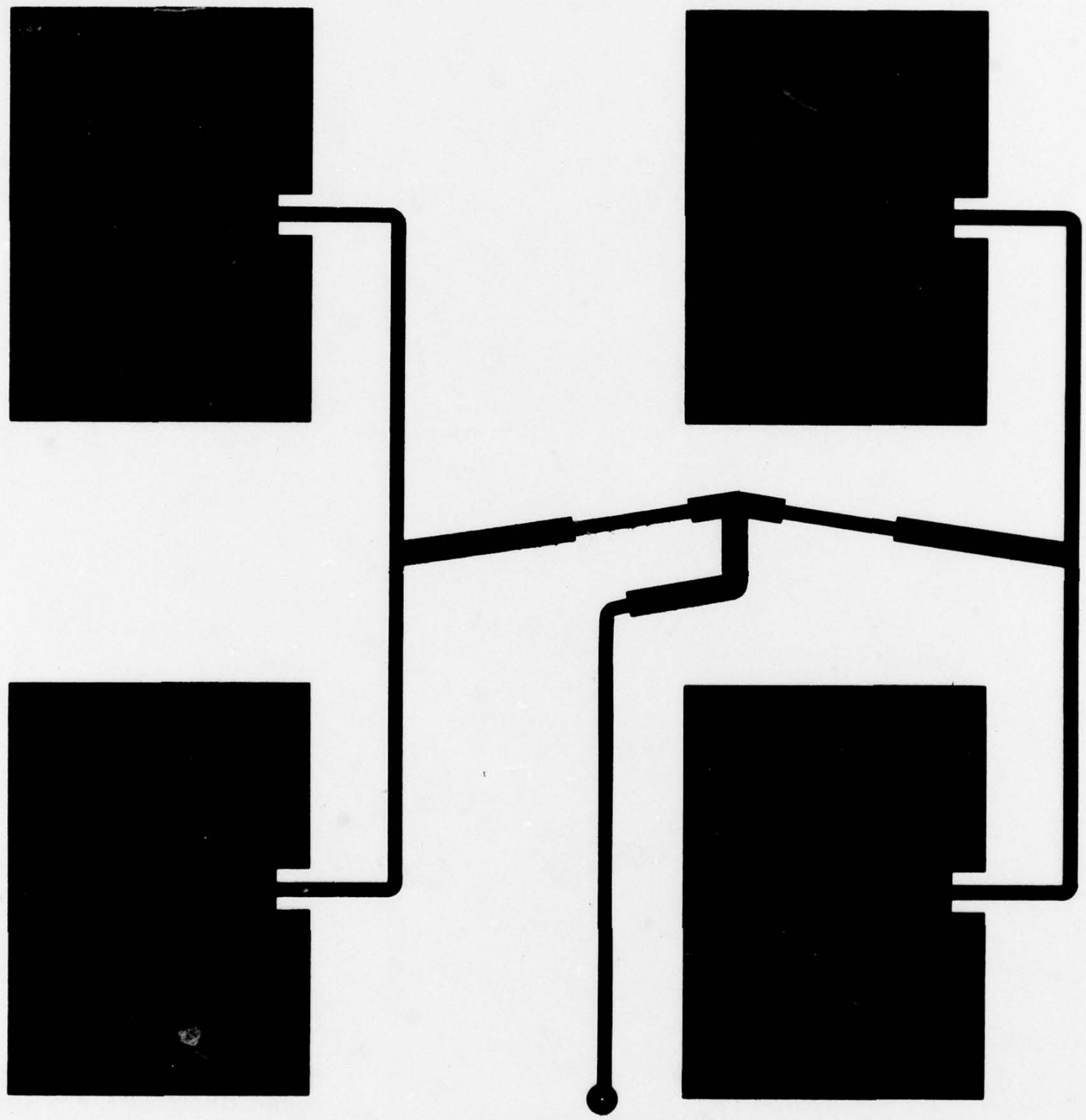

Figure 2-1 2x2 Element Array (≈1.6 x actual size)

chosen thickness at the actual operating frequency (0.005"). This ratio, .005/.063 = 0.08 was then applied to the final design frequency (0.08 * 38.4 GHz) to obtain the proper scale frequency (3.07 GHz). E and H-plane radiation patterns of the 2x2 element array are shown in Figure 2-2 and 2-3.

As part of the development process, a 4x4 element array (Figure 2-4) was fabricated and tested at a scaled frequency of 6.14 GHz on 0.031" thickness substrate material. E and H-plane radiation patterns for this array are shown in Figures 2-5 and 2-6. This array has a peak gain of approximately 18.0 dB with side-lobes down approximately -12.0 dB (standard case for a uniformly illuminated aperture).

Following is a brief analysis of array performance:

Theoretical Gain $10 \operatorname{Log}_{10} \frac{4\pi A}{\lambda^2}$	19.1 dB
Measured Gain	18.0 dB
Mismatch Loss (VSWR = 1.3:1)	0.1 dB
Actual Gain	18.1 dB

Efficiency $\approx$ 19.1 dB - 18.1 dB $\approx$ 1.0 dB $\approx$79%

This efficiency figure of 79% is commensurate with 4x4 element array results obtained during the previous contract.

A reduced side-lobe version of the previously discussed 4x4 element was designed, fabricated, and tested as the next step in the development process. The design for this array incorporated a -25 dB side-lobe Dolph-Tschebyscheff amplitude taper in both the E and H-planes. This amplitude taper is achieved by using the proper combinations of feedline impedances in the array corporate feed structure, as illustrated in Figure 2-7.

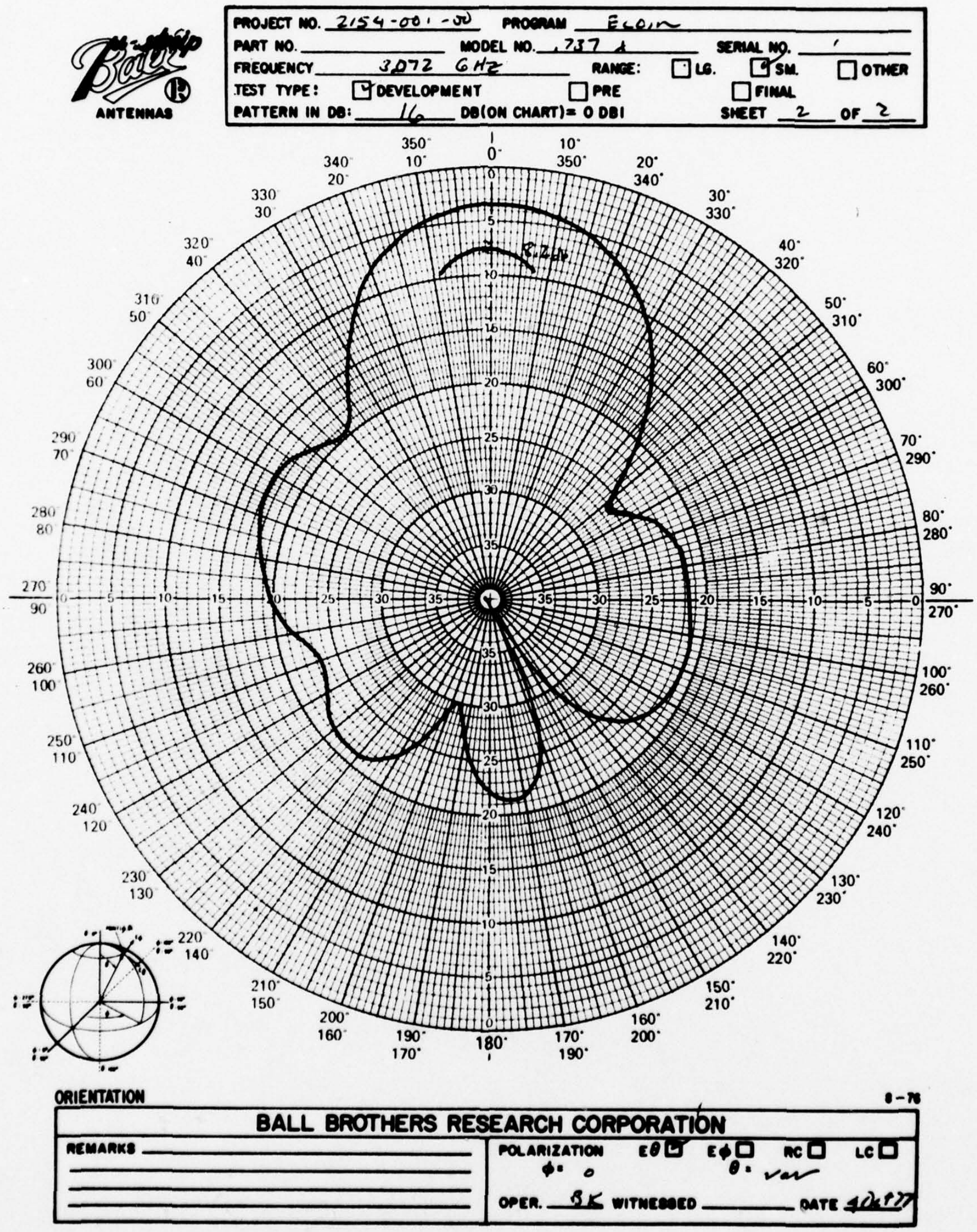

Figure 2-2 E-Plane Radiation Pattern (2x2 element array, 3.07 GHz)

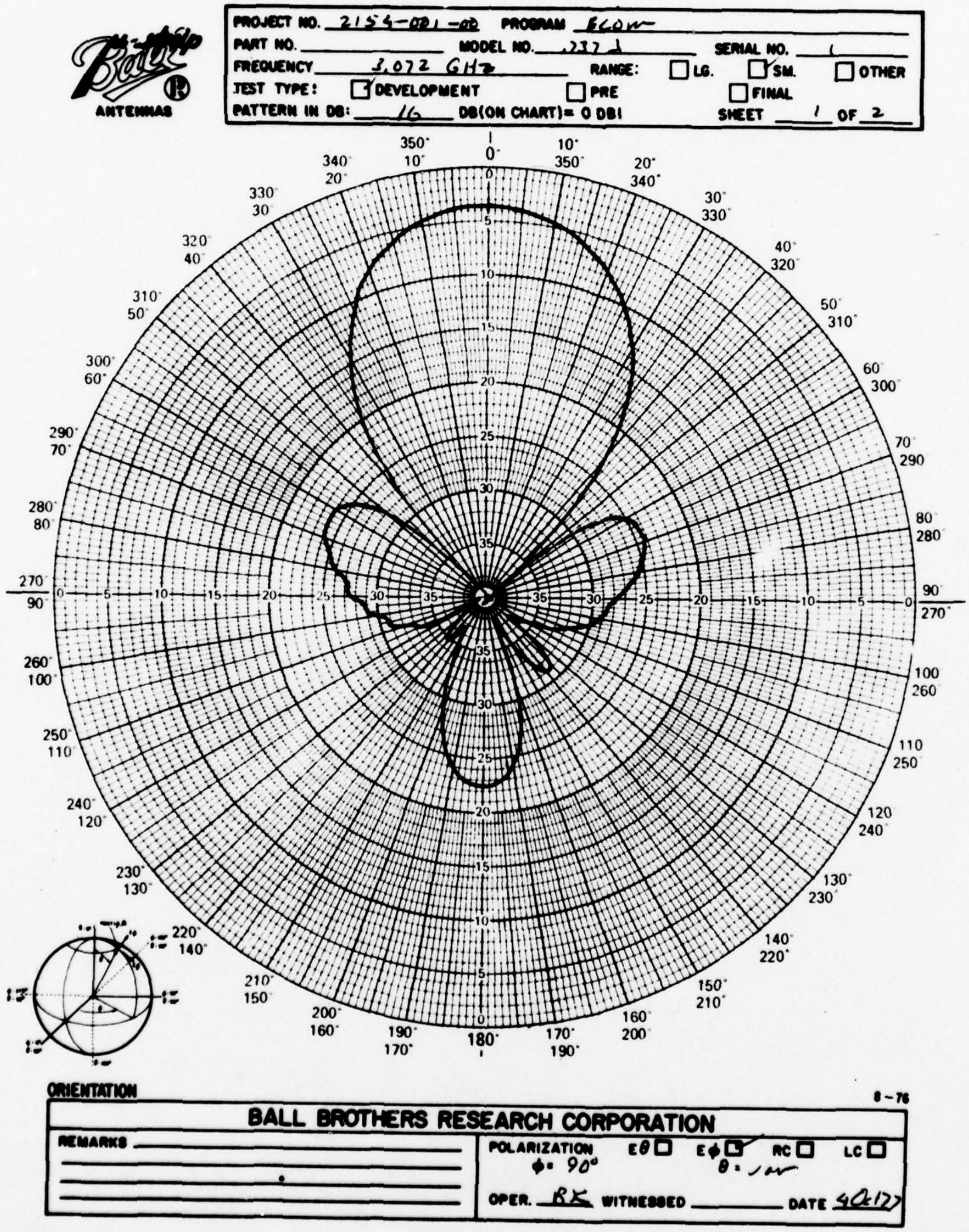

Figure 2-3 H-Plane Radiation Pattern (2x2 element array, 3.07 GHz)

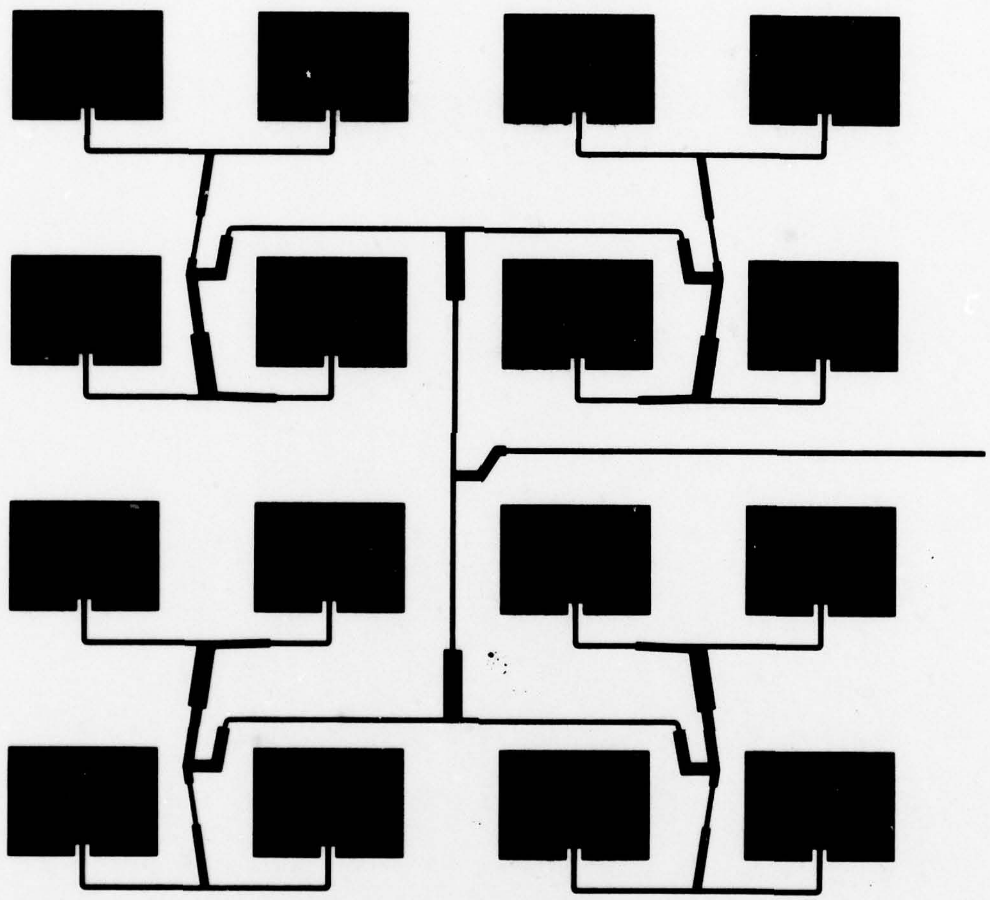

Figure 2-4 4x4 Element Array (6.14 GHz)

F78-16

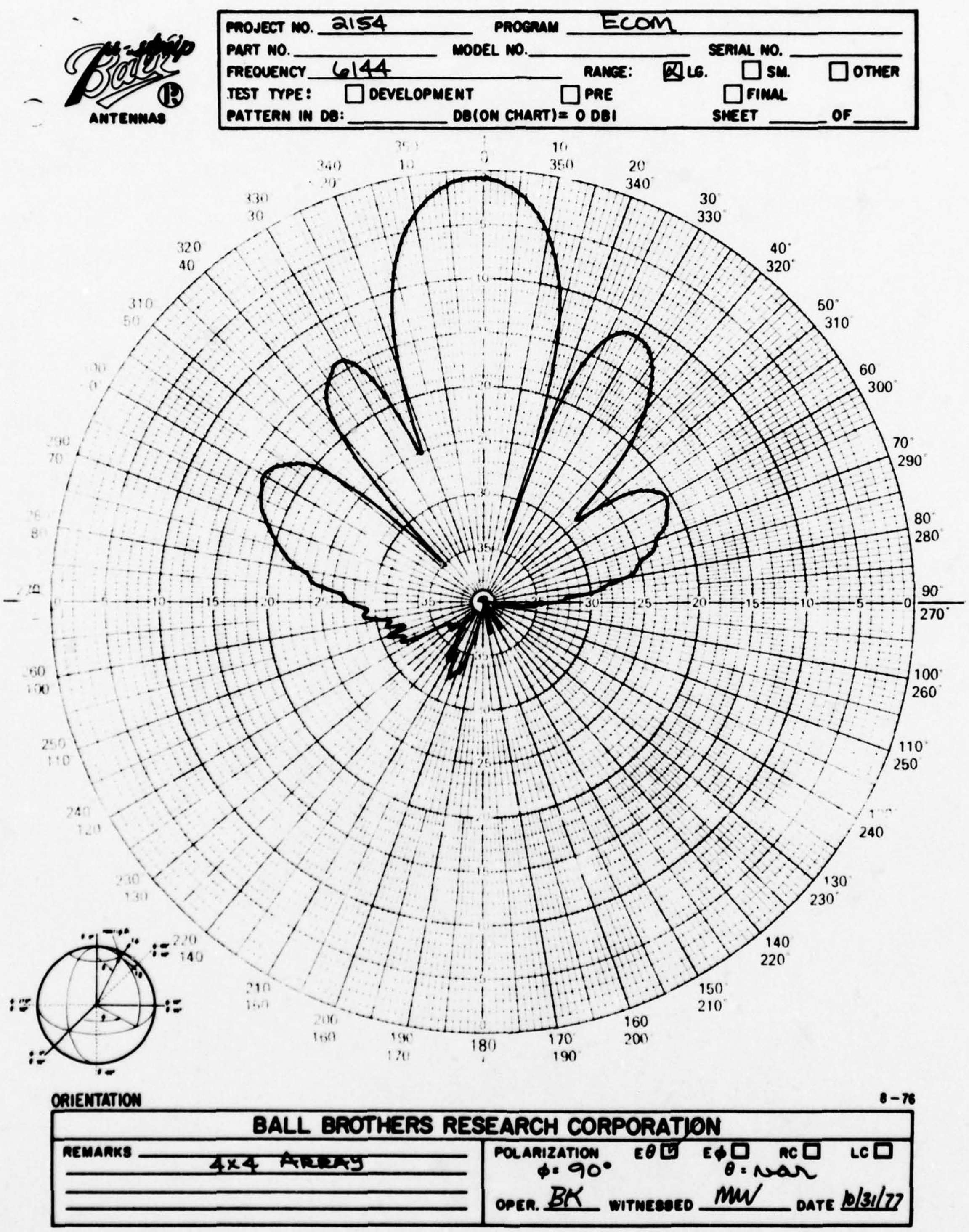

Figure 2-5 E-Plane Radiation Pattern (4x4 element array, 6.14 GHz)

F78-16 Ball

Ball ANTENNAS

PROJECT NO. 2154	PROGRAM ECOM		
PART NO.	MODEL NO.	SERIAL NO.	
FREQUENCY 6144	RANGE: ☒ LG.	☐ SM.	☐ OTHER
TEST TYPE: ☐ DEVELOPMENT	☐ PRE	☐ FINAL	
PATTERN IN DB:	DB(ON CHART)= 0 DBI	SHEET ____ OF ____	

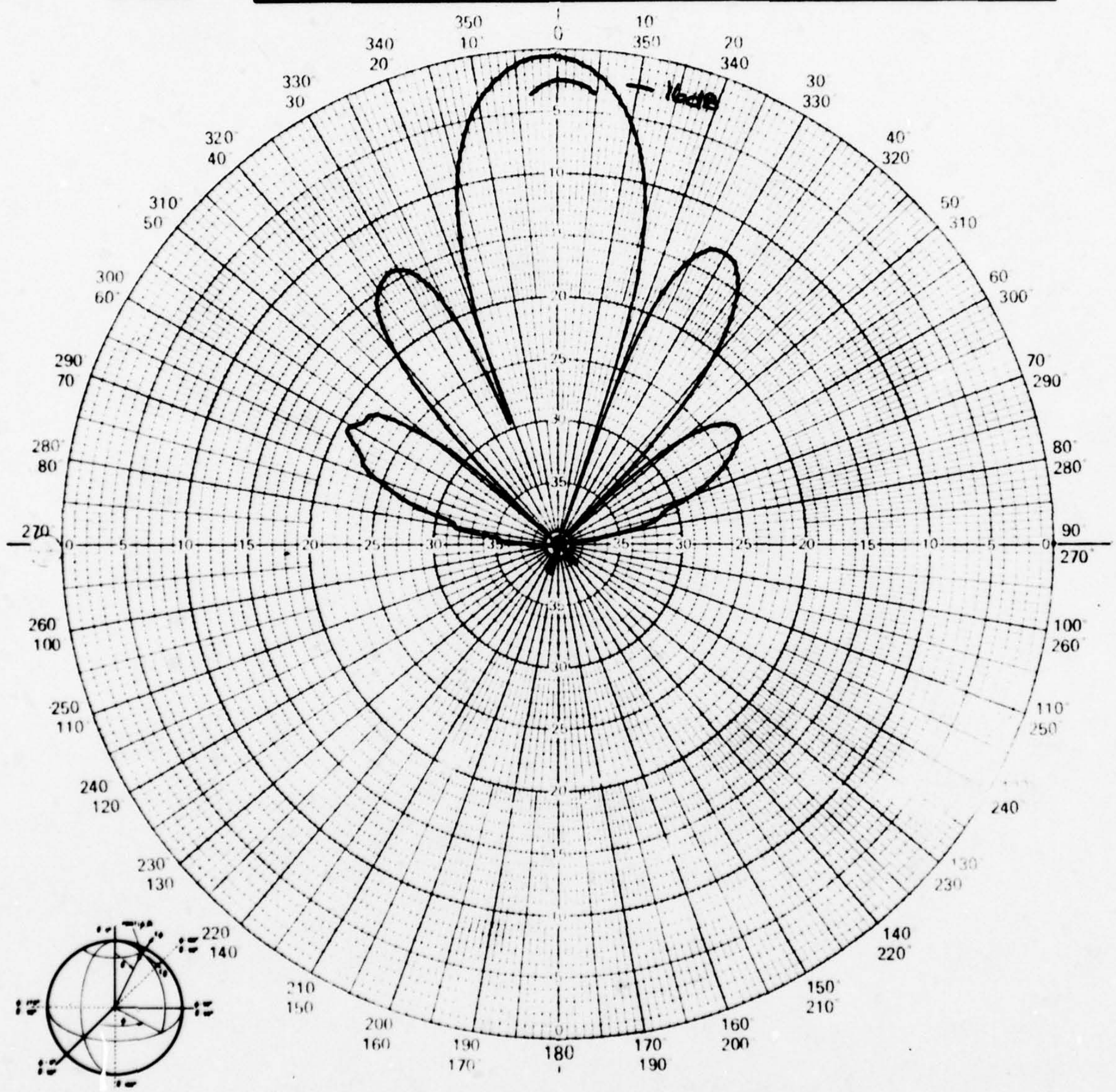

ORIENTATION

8-76

BALL BROTHERS RESEARCH CORPORATION

REMARKS 4x4 ARRAY	POLARIZATION Eθ☐ Eϕ☒ RC☐ LC☐ ϕ: 0° θ: var
	OPER. BK WITNESSED MW DATE 10/31/77

Figure 2-6 H-Plane Radiation Pattern (4x4 element array, 6.14 GHz)

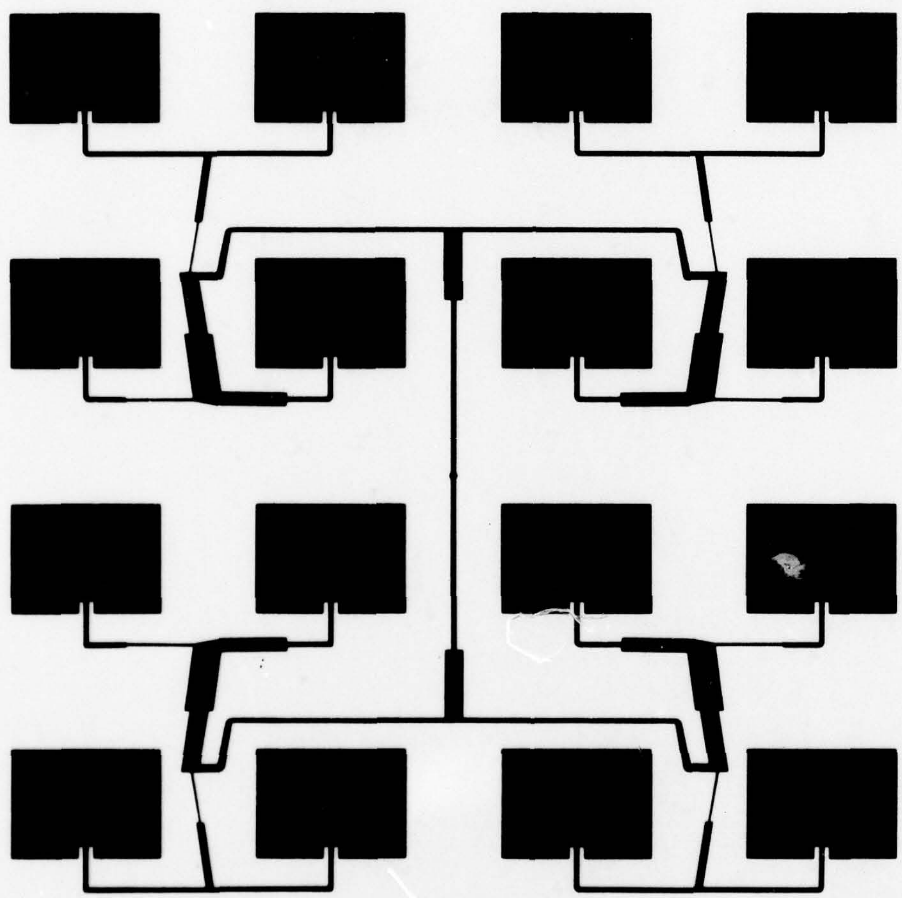

Figure 2-7 4x4 Element Reduced Side Lobe Array (6.09 GHz)

Measured E and H-plane radiation patterns of this array are shown in Figures 2-8 and 2-9. As can be seen, the side-lobe level in both cases is well below the design value of -25 dB.

Following is a brief analysis of array performance:

Theoretical Gain	19.1 dB
Measured Gain	17.2 dB
Aperture Efficiency (Loss due to amplitude taper)	0.6 dB
Mismatch Loss (VSWR = 1.9:1)	0.4 dB
Actual Gain	18.2 dB

Efficiency ≈ 19.1 dB - 18.2 dB ≈ 0.9 dB ≈ 81%

A -25 dB side-lobe Taylor taper (which is similar to the Dolph-Tschebyscheff) was chosen for the 32x32 element array. Rather than applying the amplitude taper to every element, it was applied to the previously mentioned 2x2 element "building blocks". A computer evaluation of this approach shows very little degradation over amplitude variation in every element. Figure 2-10 is a representation of the final 32x32 element array configuration.

2.3 WAVEGUIDE FEEDPLATE DESIGN

When contemplating an array of this magnitude (1024 elements) in the millimeter wavelength region, at least three problems become immediately evident.

(1) In general, the length of feedline from the input connector to any element in a corporate fed antenna is equal to one-half the sum of the length and width of the array. Therefore, as an array grows in size (number of elements), there is a corresponding increase in the feed system losses.

F78-16

PROJECT NO. 2154	PROGRAM ECOM		
PART NO.	MODEL NO.	SERIAL NO.	
FREQUENCY 6090	RANGE: ☒ LG.	☐ SM.	☐ OTHER
TEST TYPE: ☒ DEVELOPMENT	☐ PRE	☐ FINAL	
PATTERN IN DB: 17.4 DB(ON CHART) = 0 DBI	SHEET	OF	

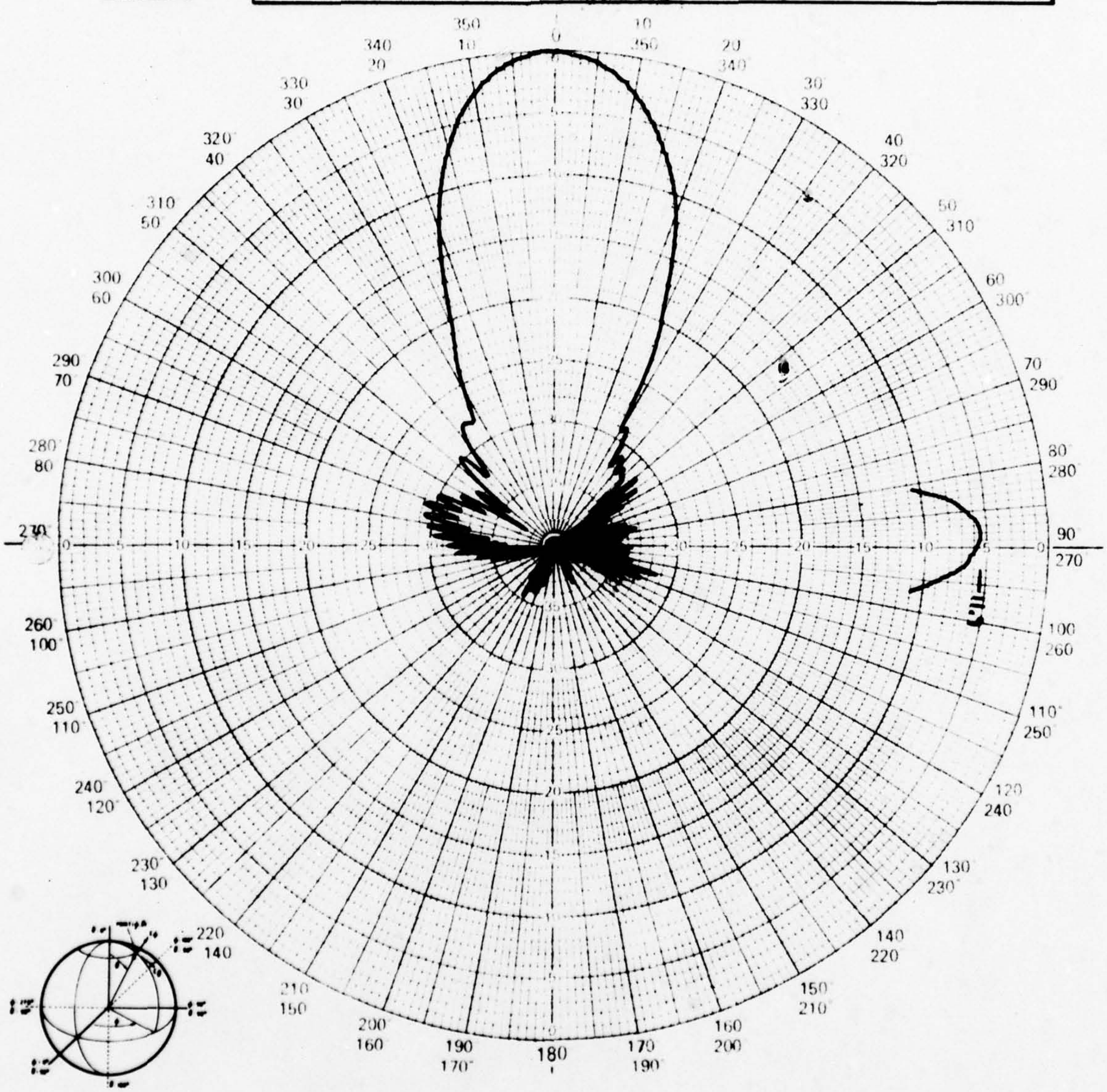

ORIENTATION

8-76

BALL BROTHERS RESEARCH CORPORATION

REMARKS 4x4 LOW SIDELOBES	POLARIZATION Eθ ☒ Eϕ ☐ RC ☐ LC ☐ ϕ: 0° θ: var OPER. MW WITNESSED MW DATE 12/2/77

Figure 2-8 E-Plane Radiation Pattern (4x4 element reduced side lobe array, 6.09 GHz)

F78-16

PROJECT NO. 2154 PROGRAM ECOM
PART NO. ______ MODEL NO. ______ SERIAL NO. ______
FREQUENCY 6090 RANGE: ☒ LG. ☐ SM. ☐ OTHER
TEST TYPE: ☒ DEVELOPMENT ☐ PRE ☐ FINAL
PATTERN IN DB: 17.4 DB(ON CHART)= 0 DBI SHEET ______ OF ______

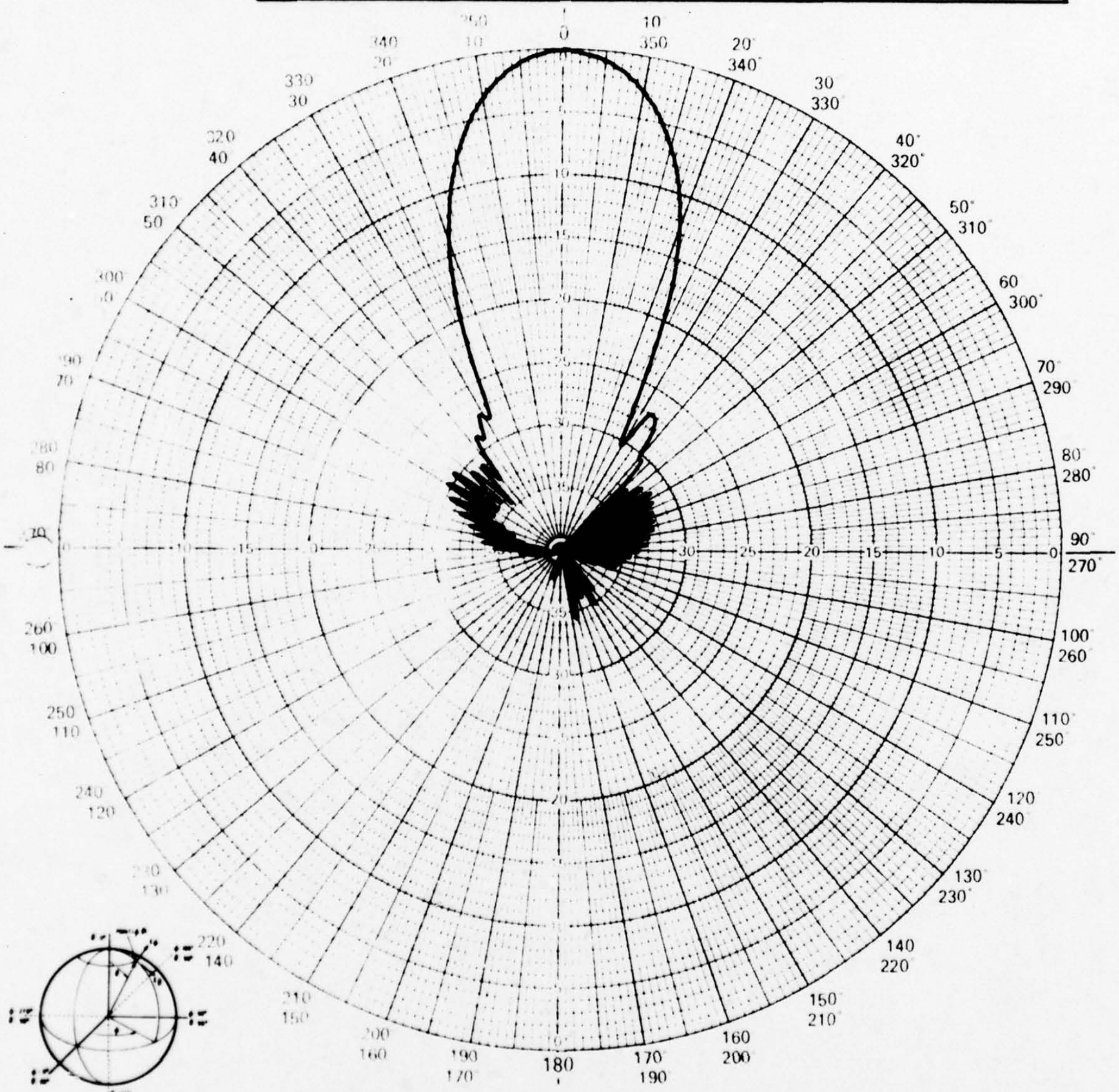

ORIENTATION 8-76

BALL BROTHERS RESEARCH CORPORATION

REMARKS 4x4 LOW SIDELOBES

POLARIZATION Eθ☐ Eφ☒ RC☐ LC☐
$\phi = 90°$ $\theta =$ var

OPER. MW WITNESSED MW DATE 12/2/77

Figure 2-9 H-Plane Radiation Pattern (4x4 element reduced side lobe array, 6.09 GHz)

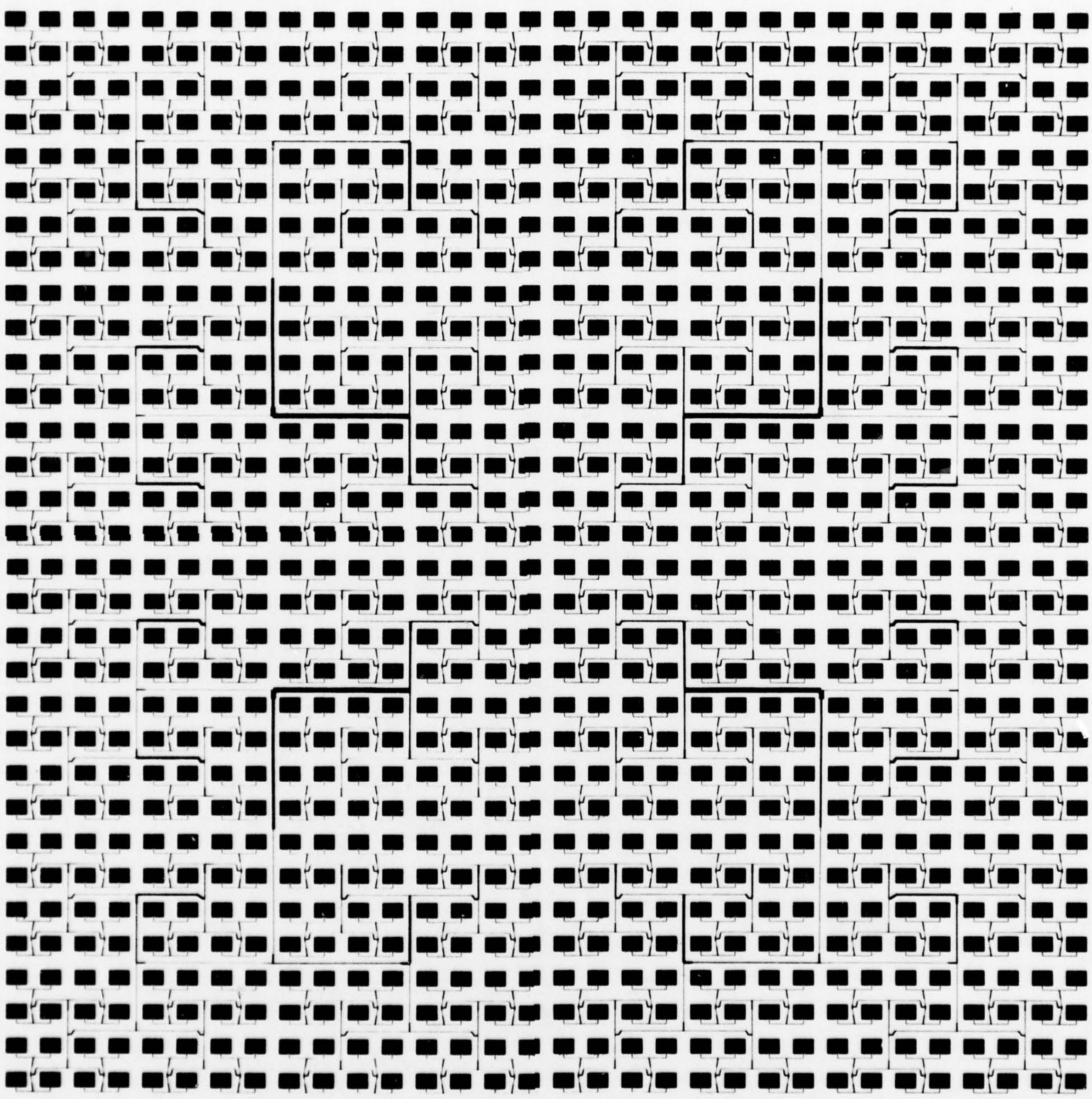

Figure 2-10 32x32 Element Reduced Side-Lobe Array (38.4 GHz)

(2) For the 32x32 element case, the power level in the two feedlines leaving the input connector is approximately 27 dB above the power level received by adjacent radiating elements. This power difference is of the order of magnitude of coupling between a radiating element and an adjacent feedline. The effect of this coupling is to disrupt amplitude and phase relationships in elements adjacent to these primary feedlines.

(3) Since the array substrate material is flexible and only 0.005" thick, it requires some type of backing plate for both support and to maintain array flatness.

The waveguide backplate, or feed plate, has been incorporated as a solution to all three of the above mentioned problems. The basic support plate referred to in (3) was chosen to be aluminum of approximately 0.25" thickness. This thickness allowed a four-way power divider to be milled into the plate in waveguide. A drawing of the feed plate layout is shown in Figure 2-11.

In effect, the first two levels of feed system power division have been converted from microstrip to waveguide. The array itself is now divided into quadrants, each of which is fed from one leg of the waveguide power divider.

This approach has the following immediate advantages:

(1) Approximately 3.4" of microstrip feedline have been replaced with waveguide. Loss is approximately 0.60 dB/in in microstrip versus less than 0.02 dB/in in waveguide. This results in a loss reduction of nearly 1.3 dB.

(2) Primary feedlines up to the third level power dividers have now been removed from the array, nearly eliminating problems with radiating element/feedline interactions.

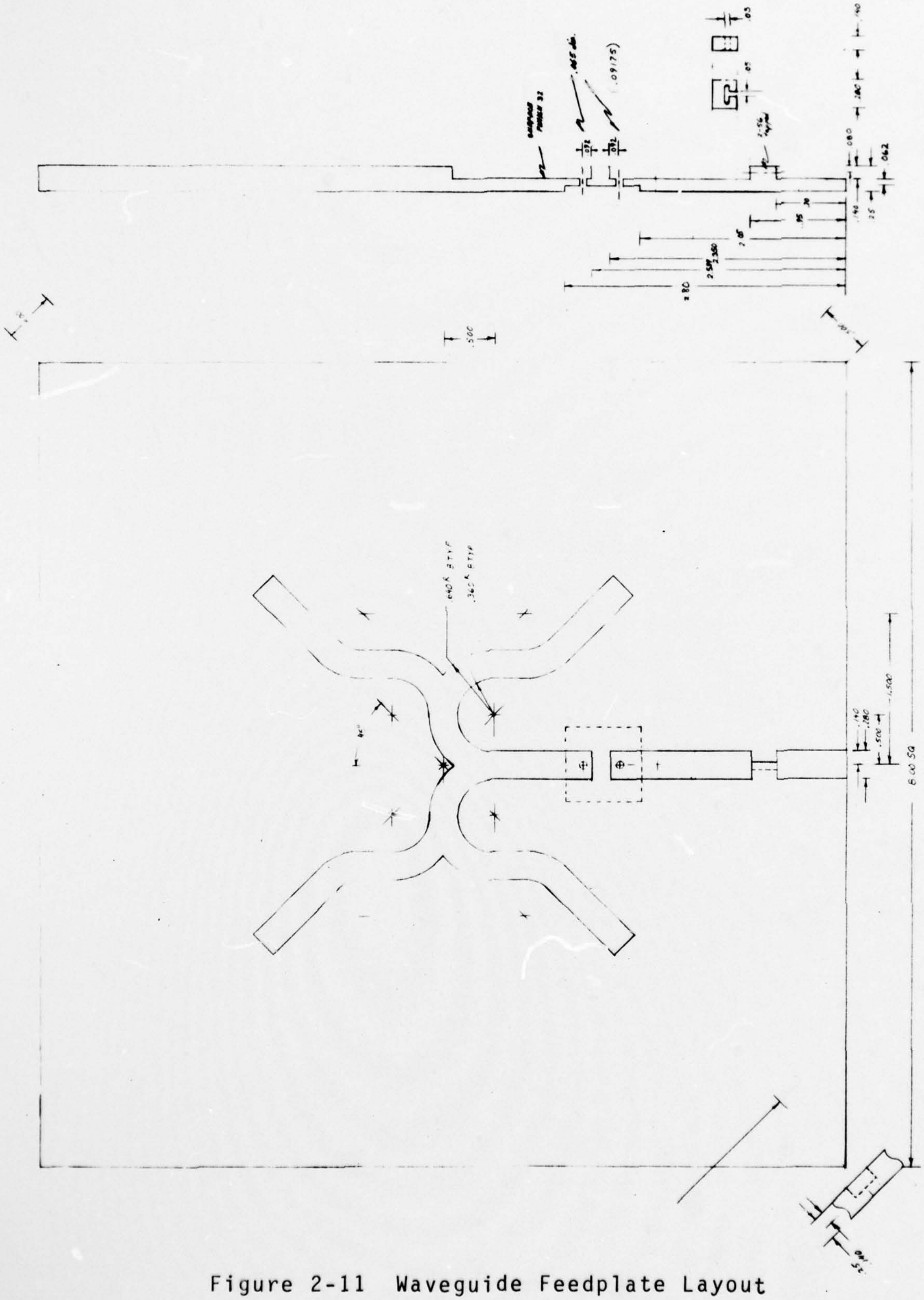

Figure 2-11 Waveguide Feedplate Layout

(3) The array substrate is provided with a rigid, flat support.

To accommodate development and testing, the array substrates delivered as part of this contract were glued to a 0.063" thick aluminum plate which was drilled and tapped so it could be screwed to the waveguide feed plate. This allowed relatively easy separation of the array from the feed plate. In future models the array substrate would be glued directly to the waveguide feed plate.

2.4 TEST RESULTS

Before fabrication of the final 32x32 element arrays at 38.4 GHz, a scaled version of the entire array was fabricated and tested. The array was etched on 0.014" thickness polyguide (similar to the Duroid substrate) and operated at 13.8 GHz.

E and H-plane radiation patterns of this array are shown in Figure 2-12. Side-lobe levels nearly meet the -20 dB design goal in both planes. It should be noted that this array did not have the waveguide-type feed system, but was fed entirely with a microstrip corporate feed network. Measured gain of the entire array was 24 dB. This low value was later discovered to be the result of a bad test cable. The gain measurement could not be repeated as part of the array feed system had been removed to perform tests on one-half of the array.

Figure 2-13 shows E and H-plane patterns for one-half (16x32 elements) of the array. In this case, measured gain is 28.0 dB for one-half the array.

Following is an analysis of array performance:

Theoretical Gain	38.0 dB
Measured Gain (½ array)	28.0 dB
Other Half of Array	3.0 dB
Aperture Efficiency	0.9 dB
Mismatch Loss (VSWR = 2.0:1)	0.5 dB
Actual Gain	32.4 dB

Efficiency ≈ 38.0 dB - 32.4 dB ≈ 5.6 dB ≈ 28%

F78-16

Ball ANTENNAS

PROJECT NO. 2154	PROGRAM ECOM		
PART NO.	MODEL NO.	SERIAL NO.	
FREQUENCY 13.795 GHz	RANGE: ☑ LG.	☐ SM.	☐ OTHER
TEST TYPE: ☐ DEVELOPMENT	☐ PRE	☐ FINAL	
PATTERN IN DB:	DB(ON CHART)= 0 DBI	SHEET	OF

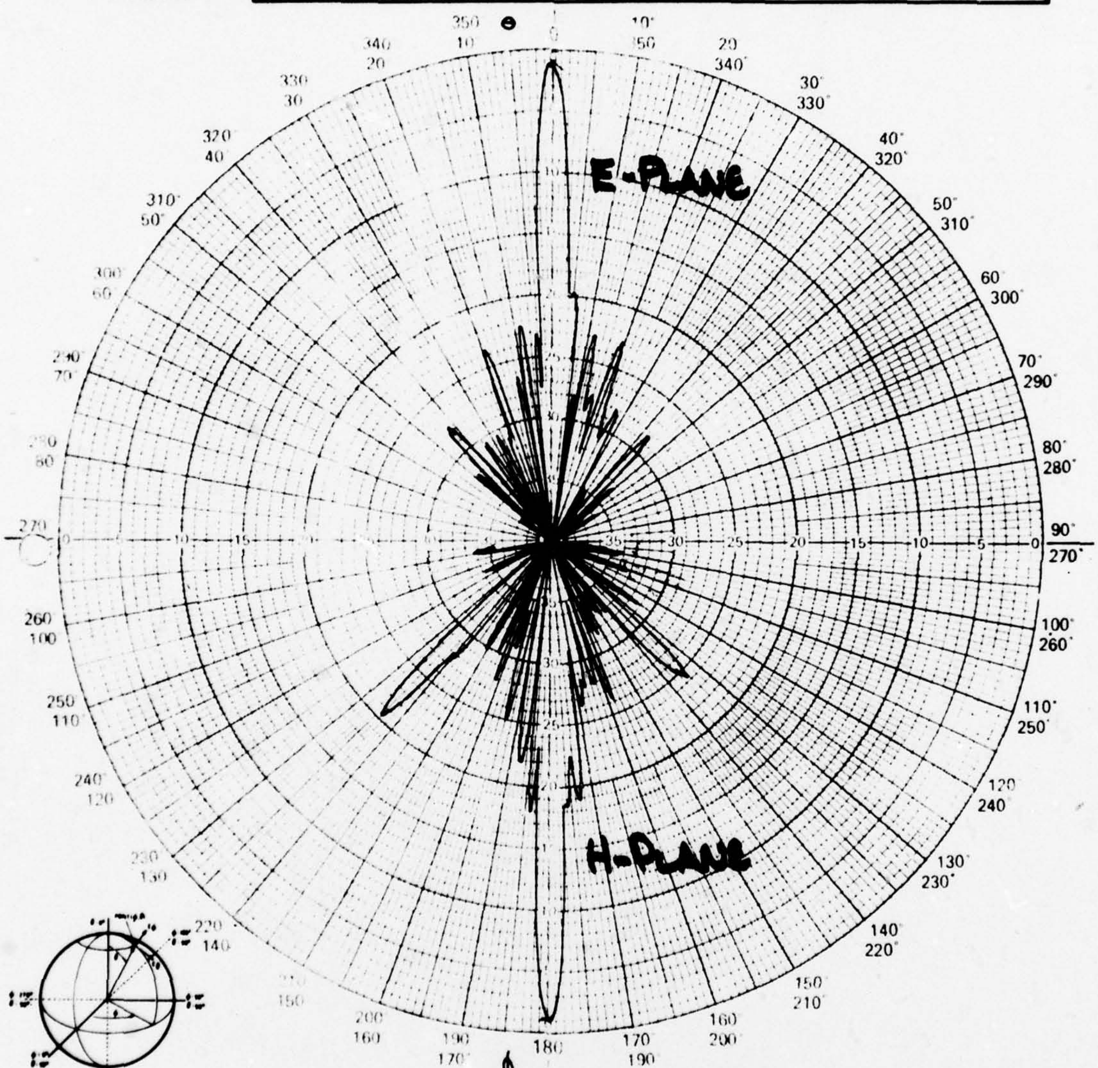

ORIENTATION

8-76

BALL BROTHERS RESEARCH CORPORATION

REMARKS	POLARIZATION Eθ ☒ Eφ ☒ RC ☐ LC ☐ φ = 0, 90° θ = var
	OPER. BK WITNESSED MW DATE 4/12/78

Figure 2-12 E and H-Plane Radiation Patterns (32x32 element array, 13.8 GHZ)

F78-16 Ball

Ball Antennas

PROJECT NO. 2154 PROGRAM ECOM
PART NO. ____ MODEL NO. ____ SERIAL NO. ____
FREQUENCY 13.80 GHz RANGE: [X] LG. [ ] SM. [ ] OTHER
TEST TYPE: [ ] DEVELOPMENT [ ] PRE [ ] FINAL
PATTERN IN DB: ____ DB(ON CHART)= 0 DBI SHEET ____ OF ____

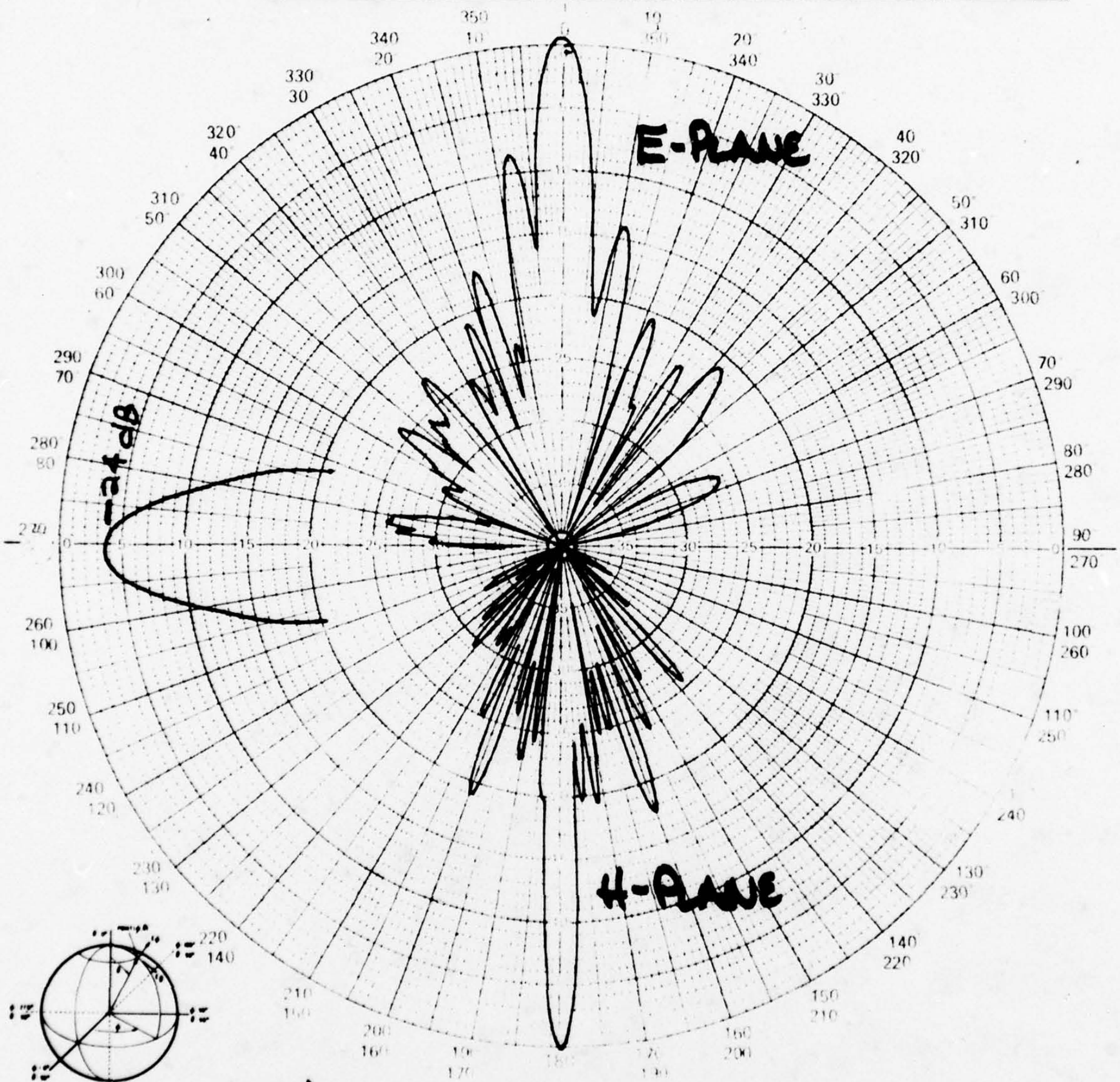

ORIENTATION HALF ARRAY 8-76

BALL BROTHERS RESEARCH CORPORATION

REMARKS ____

POLARIZATION Eθ [X] Eφ [X] RC [ ] LC [ ]
φ: θ:
OPER. BK WITNESSED MW DATE 4/18/78

Figure 2-13 E and H-Plane Radiation Patterns
(16x32 element array, 13.8 GHz)

Figures 2-14 and 2-15 are front and back views of the final array operating at 38.4 GHz. Two units (Model AN152A, Serial Numbers 001 and 002) were delivered. Input VSWRs of the two antennas are presented in Table 2-1.

Table 2-1

INPUT VSWRs OF MODEL AN152A
SERIAL NUMBERS 001 and 002

Freq (GHz)	Serial #001 VSWR	Serial #002 VSWR
38.340	2.50:1	1.53:1
38.355	2.25:1	1.51:1
38.370	2.15:1	1.55:1
38.385	2.10:1	1.55:1
38.400	2.00:1	1.60:1
38.415	1.97:1	1.64:1
38.430	1.95:1	1.67:1
38.445	1.95:1	1.71:1
38.460	2.00:1	1.78:1

Measured E and H-plane radiation patterns of Serial Numbers 001 and 002 at frequencies of 38.0/38.1, 38.4 and 38.7 GHz are shown in Figures 16 through 27. Gain values for S/N 001 and 002 at 38.4 GHz are 29 dB and 25 dB respectively.

Although the measured gain of S/N 001 nearly meets the design goal, side-lobe levels do not approach the -20 dB goal. When S/N 002 was first tested, general pattern shape and side-lobe level was much worse than S/N 001. The radiation patterns shown in Figures 2-22 through 2-27 are the result of an attempt to "retune" the array by placing pieces of teflon tape on certain parts of the feed structure. The tape effectively changes the impedance and phase relationships of the feed network. As can be seen, this "retune" had the effect of achieving the desired pattern in the H-plane.

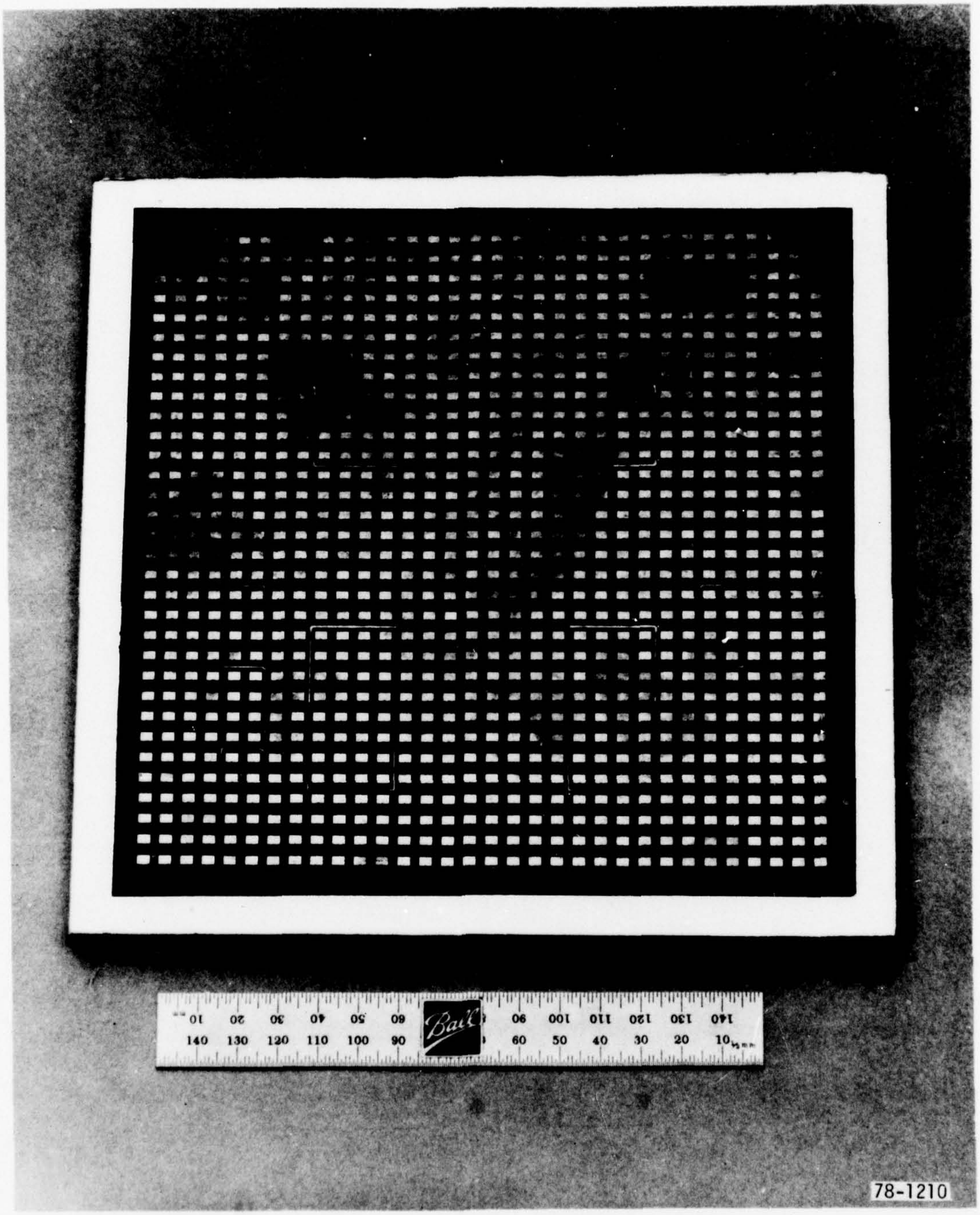

Figure 2-14 Front View of 32x32 Element Reduced Side Lobe Array (38.4 GHz)

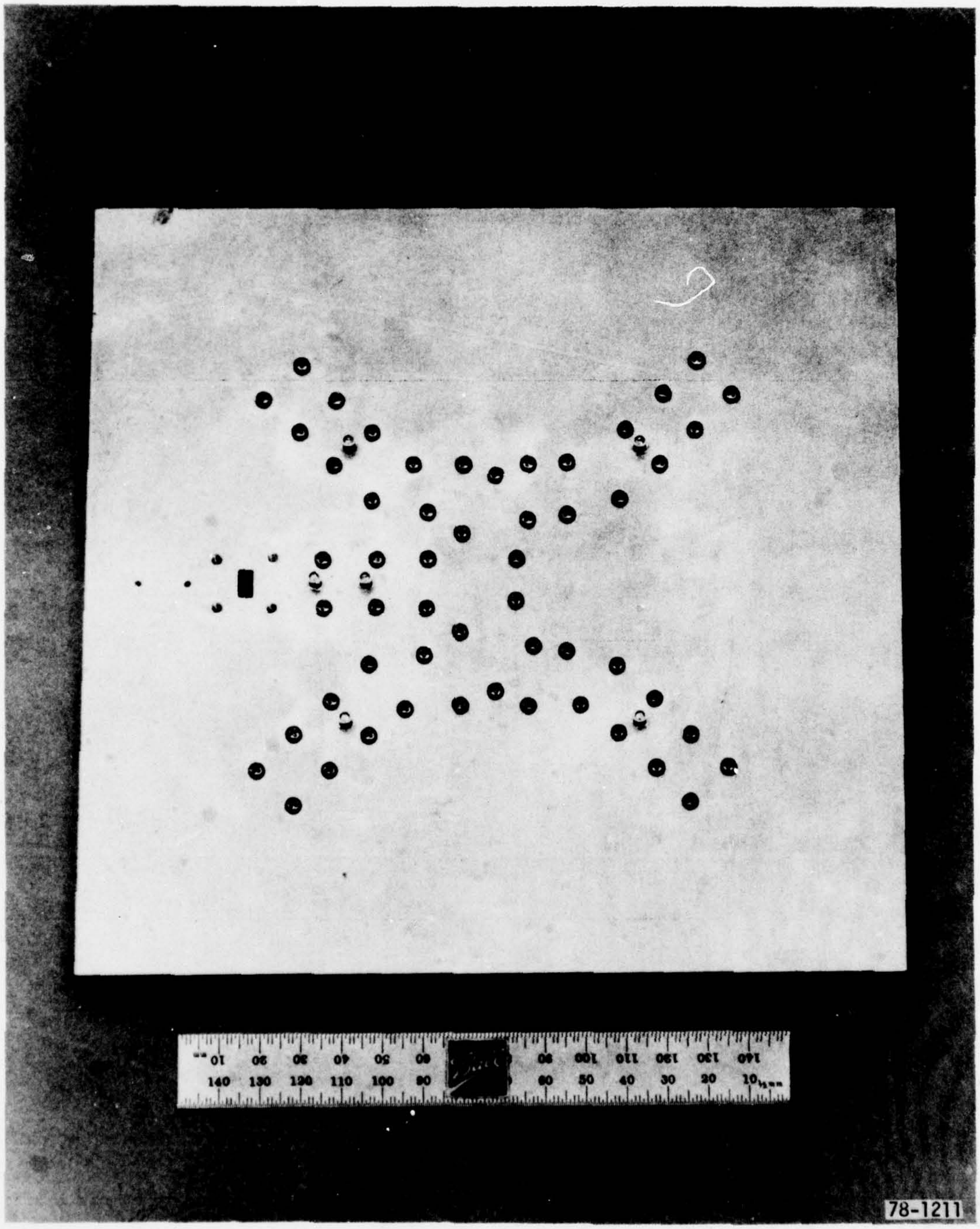

Figure 2-15 Back View of 32x32 Element Array (38.4 GHz)

F78-16

Ball ANTENNAS

PROJECT NO. 2154	PROGRAM ECOM		
PART NO.	MODEL NO. I A (ANIS2A)	SERIAL NO. 001	
FREQUENCY 38.0 GHz	RANGE: ☑ LG.	☒ SM.	☐ OTHER
TEST TYPE: ☐ DEVELOPMENT	☐ PRE	☒ FINAL	
PATTERN IN DB: 28	DB(ON CHART)= 0 DBI	SHEET ____ OF ____	

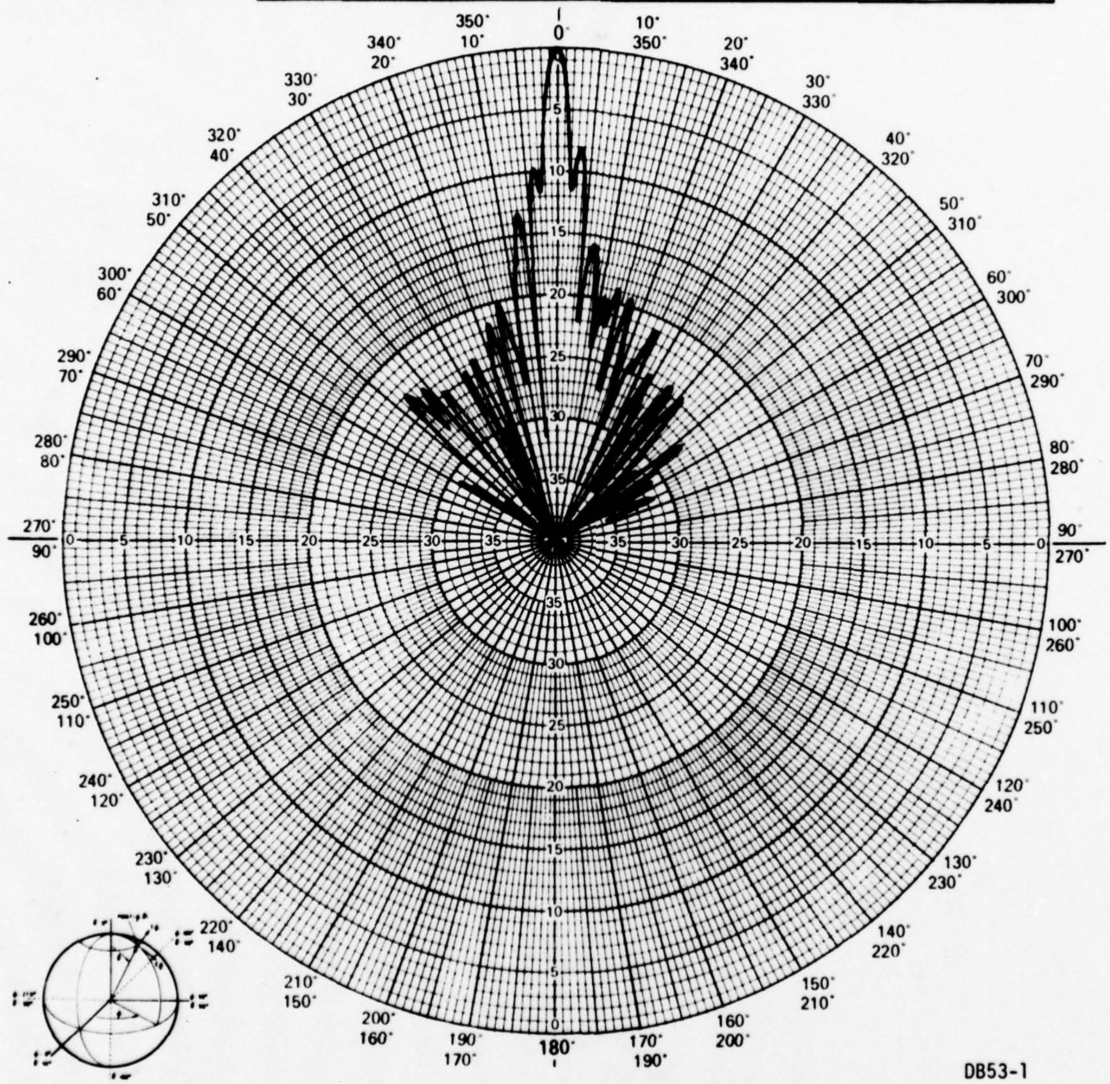

DB53-1
6/78

ORIENTATION

BALL AEROSPACE SYSTEMS DIVISION

REMARKS	POLARIZATION
E-PLANE	Eθ ■ Eφ ☐ RC ☐ LC ☐ φ= θ=
	OPER. MAW WITNESSED MAW DATE 8/23/8

Figure 2-16 E-Plane Radiation Pattern (Serial #001, 38.0 GHz)

F78-16

BALL ANTENNAS

PROJECT NO. 2154 PROGRAM ECOM

PART NO. ______ MODEL NO. I A(AN152A) SERIAL NO. 001

FREQUENCY 38.4 GHz RANGE: ☐ LG. ☒ SM. ☐ OTHER

TEST TYPE: ☐ DEVELOPMENT ☐ PRE ☒ FINAL

PATTERN IN DB: 29 DB(ON CHART)= 0 DBI SHEET ______ OF ______

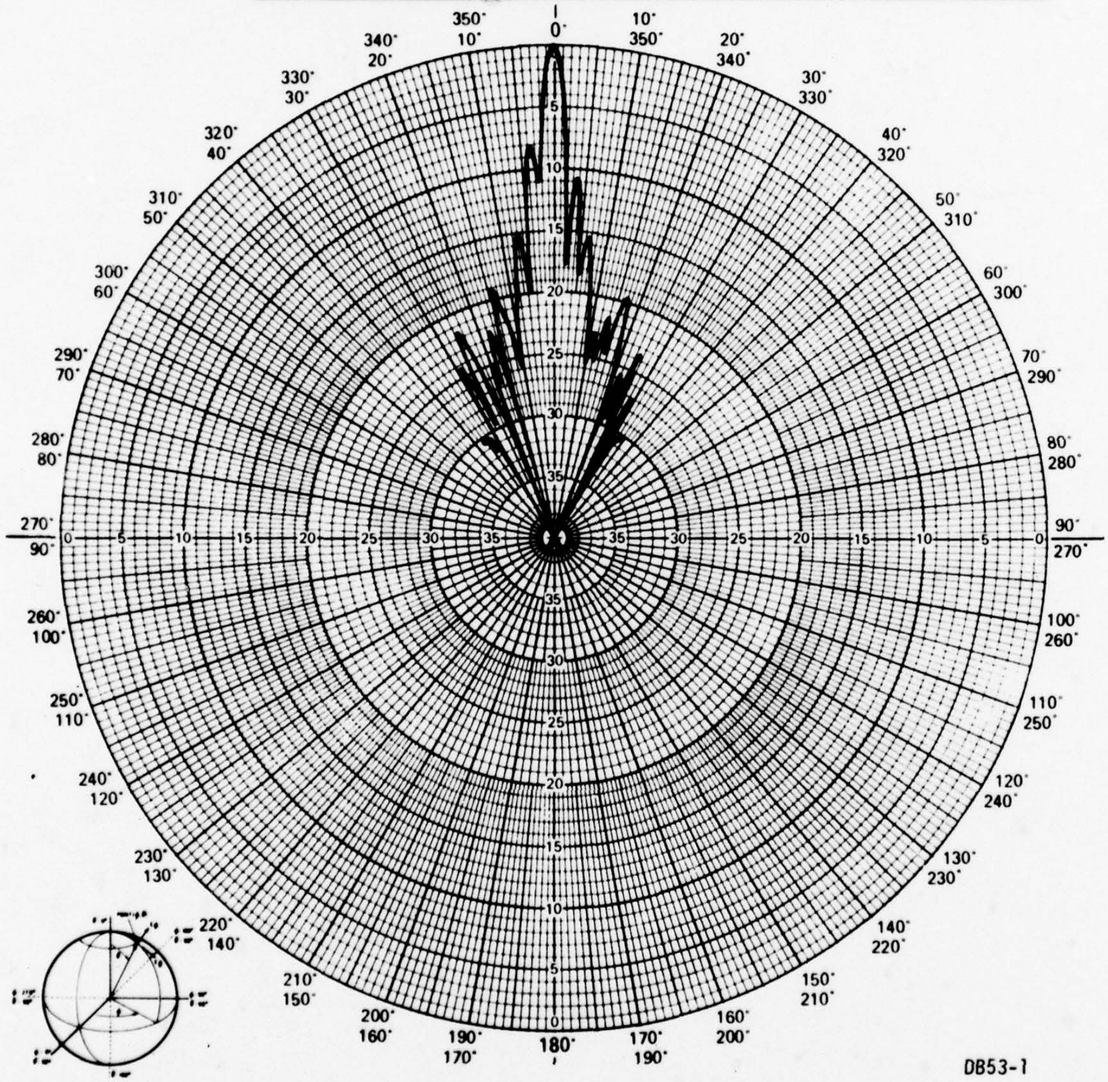

ORIENTATION

DB53-1
6/78

BALL AEROSPACE SYSTEMS DIVISION

REMARKS	POLARIZATION Eθ ☒ Eϕ ☐ RC ☐ LC ☐
E-PLANE	ϕ: θ:
	OPER. MW WITNESSED MW DATE 9/23/78

Figure 2-17 E-Plane Radiation Pattern (Serial #001, 38.4 GHz)

F78-16 Ball

Ball ANTENNAS

PROJECT NO. 2154 PROGRAM ECOM

PART NO. ______ MODEL NO. IA (ANIS2A) SERIAL NO. 001

FREQUENCY 38.7 GHz RANGE: ☐ LG. ☒ SM. ☐ OTHER

TEST TYPE: ☐ DEVELOPMENT ☐ PRE ☒ FINAL

PATTERN IN DB: 37 DB(ON CHART) = 0 DBI SHEET ______ OF ______

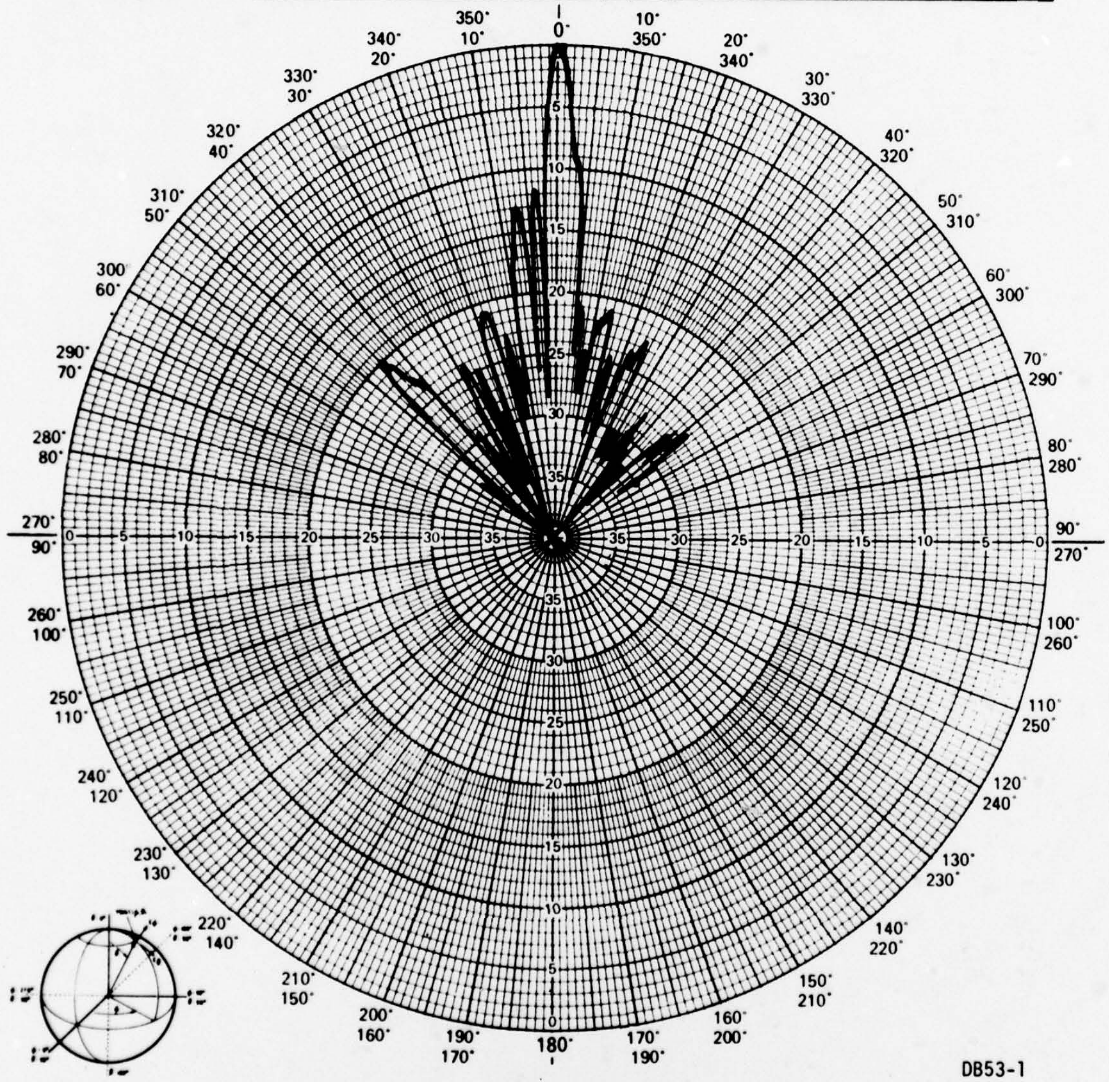

ORIENTATION

DB53-1
6/78

BALL AEROSPACE SYSTEMS DIVISION

REMARKS E-PLANE

POLARIZATION Eθ ☒ Eφ ☐ RC ☐ LC ☐
φ: θ:

OPER. MW WITNESSED MW DATE 8/23/8

Figure 2-18 E-Plane Radiation Pattern (Serial #001, 38.7 GHz)

F78-16

PROJECT NO. 2154	PROGRAM ECOM
PART NO.	MODEL NO. I A (ANISZA) SERIAL NO. 001
FREQUENCY 38.0 GHz	RANGE: ☐ LG. ☒ SM. ☐ OTHER
TEST TYPE: ☐ DEVELOPMENT	☐ PRE ☒ FINAL
PATTERN IN DB: 28	DB(ON CHART)= 0 DBI SHEET ___ OF ___

ANTENNAS

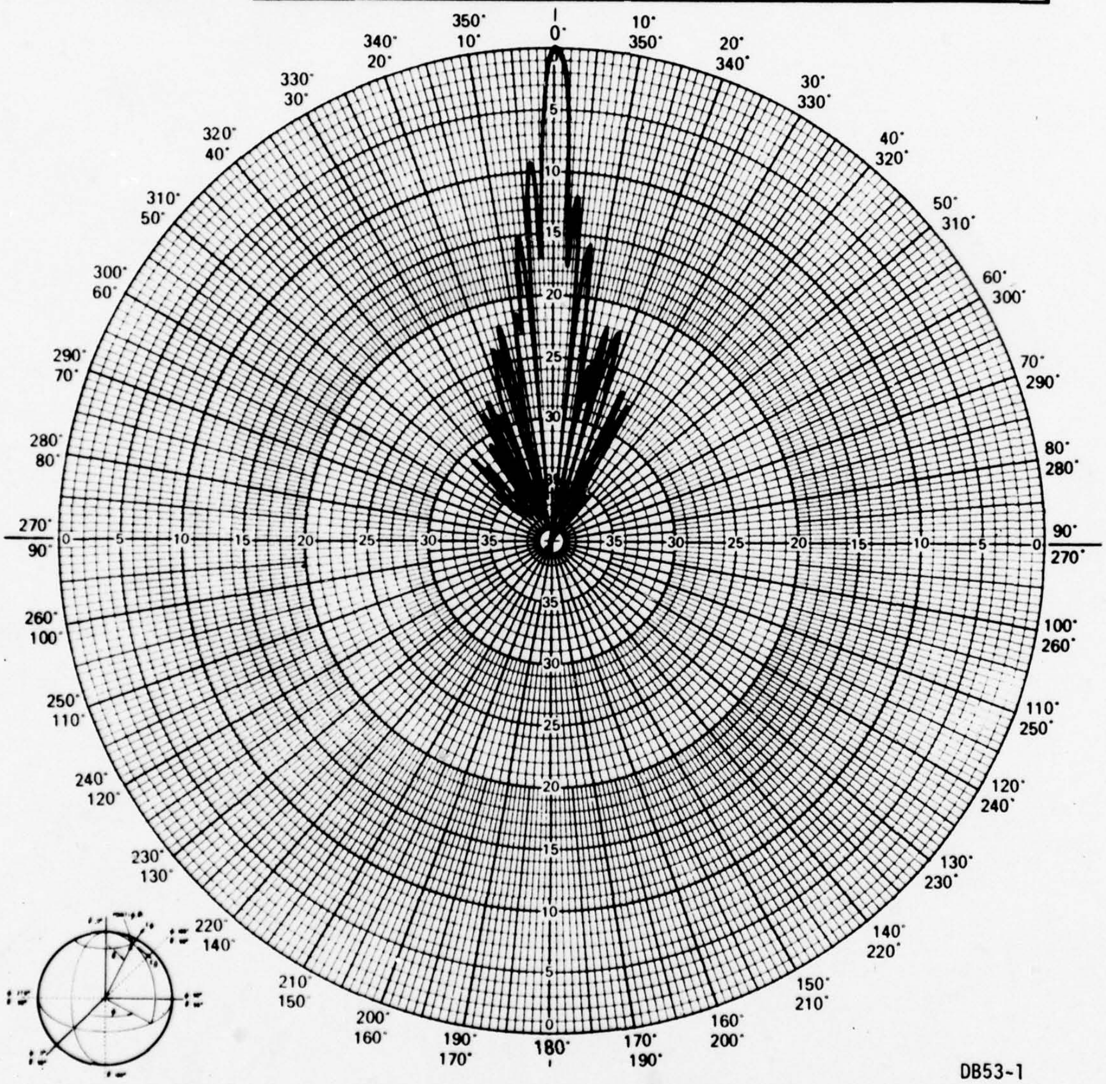

ORIENTATION

DB53-1
6/78

BALL AEROSPACE SYSTEMS DIVISION

REMARKS H-PLANE	POLARIZATION Eθ☐ Eφ☒ RC☐ LC☐ φ= θ=
	OPER. MW WITNESSED MW DATE 8/23/78

Figure 2-19 H-Plane Radiation Pattern (Serial #001, 38.0 GHz)

F78-16

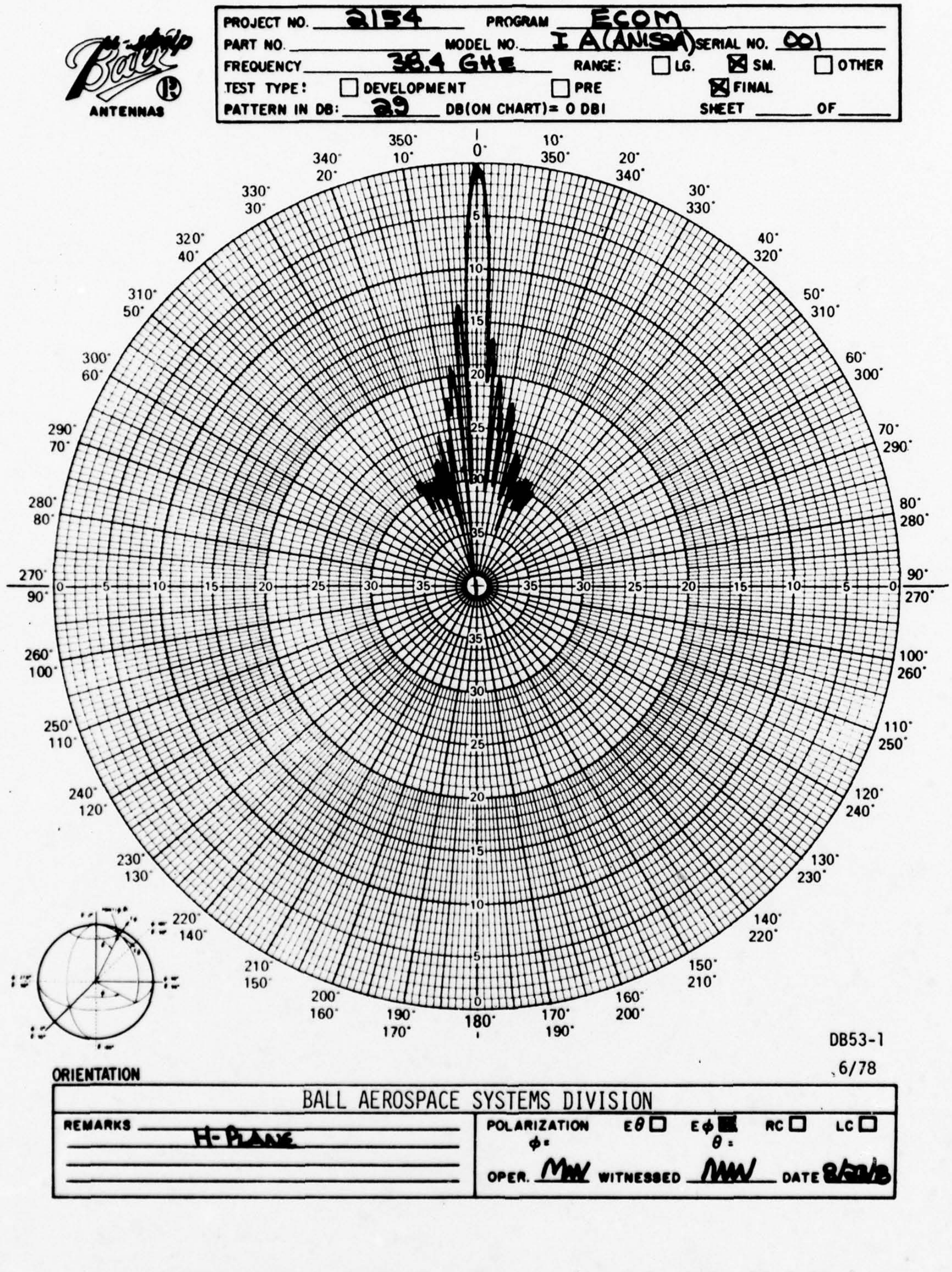

Figure 2-20 H-Plane Radiation Pattern (Serial #001, 38.4 GHz)

PROJECT NO. 2154 PROGRAM ECOM

PART NO. ______ MODEL NO. I A (ANIGA) SERIAL NO. 001

FREQUENCY 38.7 GHz RANGE: ☐ LG. ☒ SM. ☐ OTHER

TEST TYPE: ☐ DEVELOPMENT ☐ PRE ☒ FINAL

PATTERN IN DB: 27 DB(ON CHART)= 0 DBI SHEET ______ OF ______

ANTENNAS

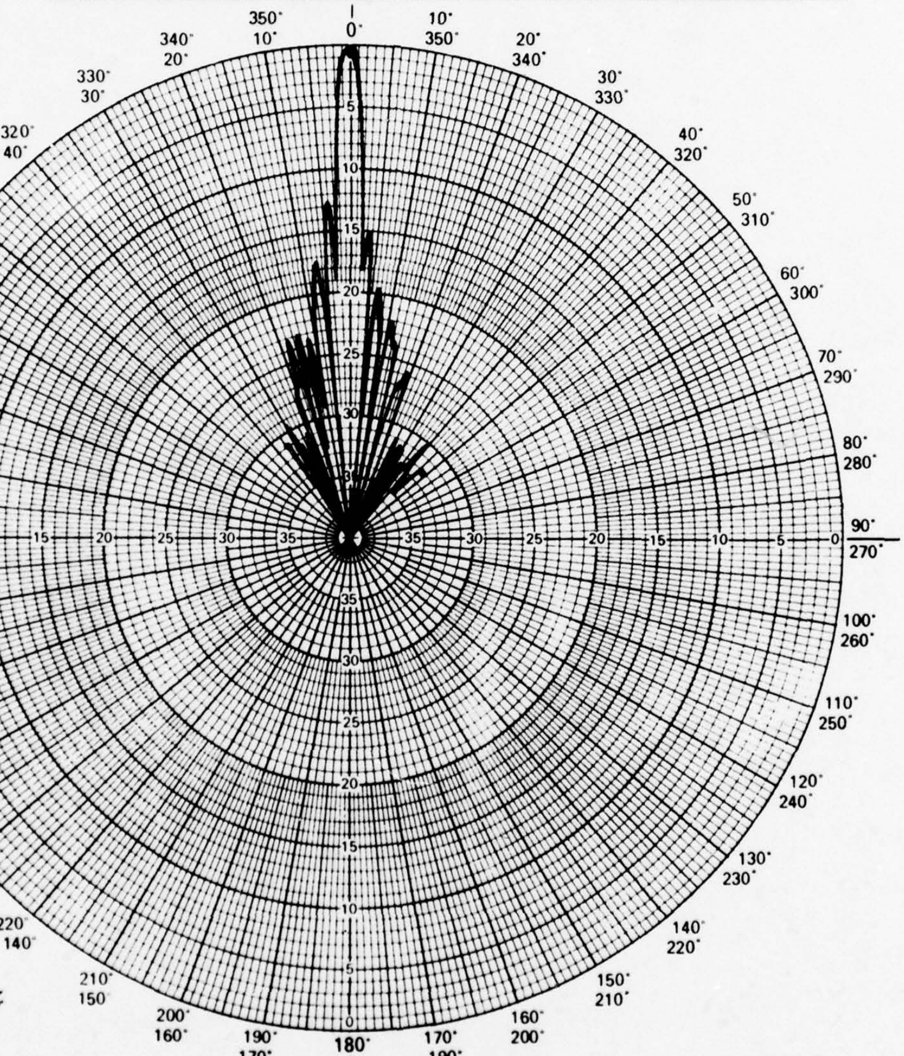

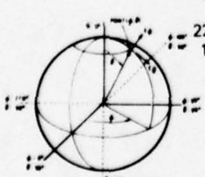

DB53-1

6/78

ORIENTATION

BALL AEROSPACE SYSTEMS DIVISION

REMARKS H- PLANE

POLARIZATION Eθ☐ Eφ☒ RC☐ LC☐

φ = θ =

OPER. MW WITNESSED MW DATE 8/23/8

Figure 2-21 H-Plane Radiation Pattern (Serial #001, 38.7 GHz)

F78-16

Ball

Ball ANTENNAS

PROJECT NO. 2154 PROGRAM ECOM

PART NO. ______ MODEL NO. AN152 A SERIAL NO. 002

FREQUENCY 38.1 GHz RANGE: ☐ LG. ☒ SM. ☐ OTHER

TEST TYPE: ☐ DEVELOPMENT ☐ PRE ☒ FINAL

PATTERN IN DB: 25 DB(ON CHART)= 0 DBI SHEET ______ OF ______

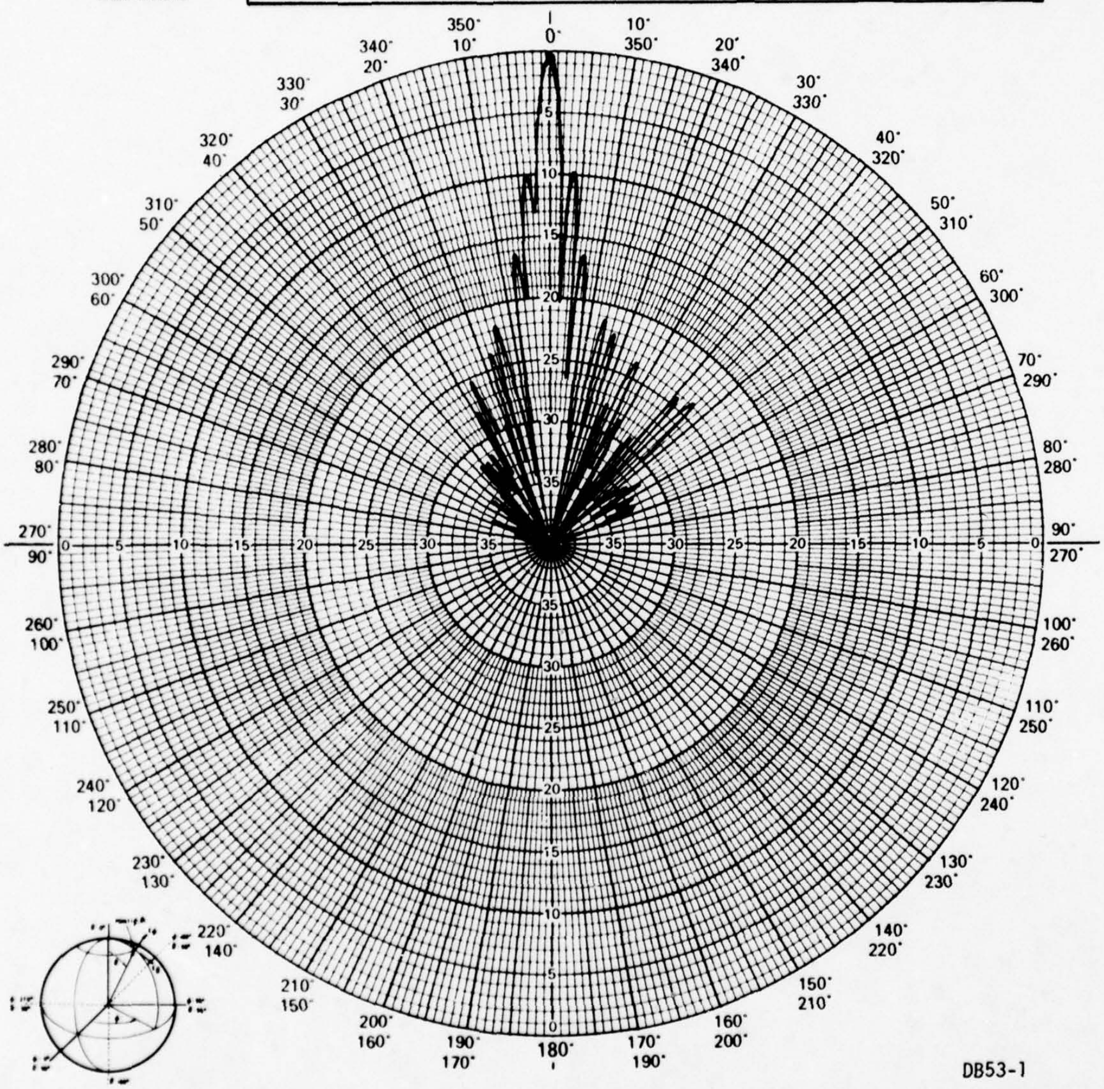

ORIENTATION

DB53-1
6/78

BALL AEROSPACE SYSTEMS DIVISION

REMARKS E-PLANE	POLARIZATION Eθ ☒ Eϕ ☐ RC ☐ LC ☐ ϕ= θ= OPER. MW WITNESSED MW DATE 8/31/78

Figure 2-22 E-Plane Radiation Pattern (Serial #002, 38.1 GHz)

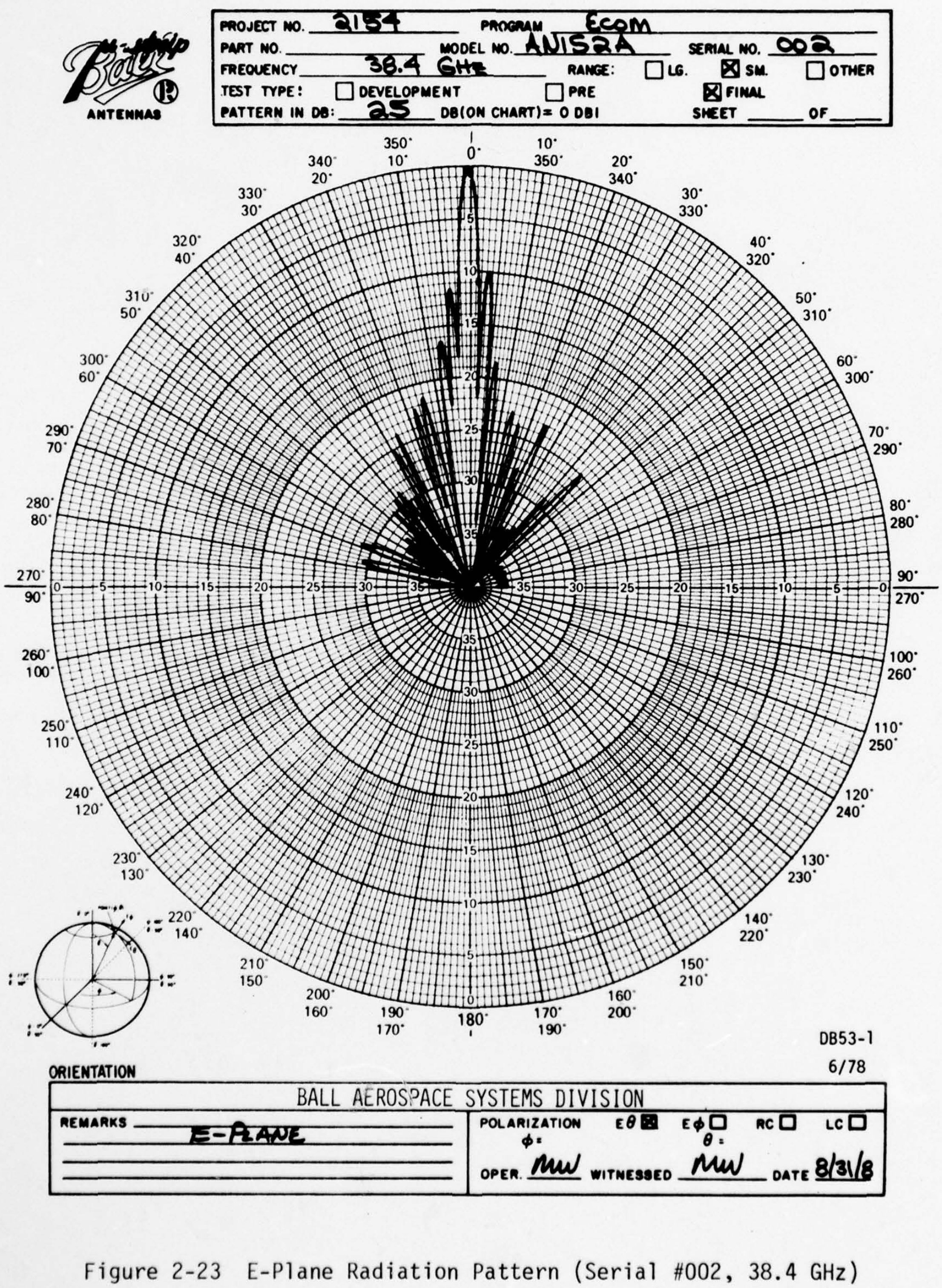

Figure 2-23 E-Plane Radiation Pattern (Serial #002, 38.4 GHz)

F78-16

ANTENNAS

PROJECT NO. 2154	PROGRAM ECOM		
PART NO. ______	MODEL NO. AN152A	SERIAL NO. 002	
FREQUENCY 38.7 GHz	RANGE: ☐ LG.	☒ SM.	☐ OTHER
TEST TYPE: ☐ DEVELOPMENT	☐ PRE	☒ FINAL	
PATTERN IN DB: 23	DB(ON CHART)= 0 DBI	SHEET ______ OF ______	

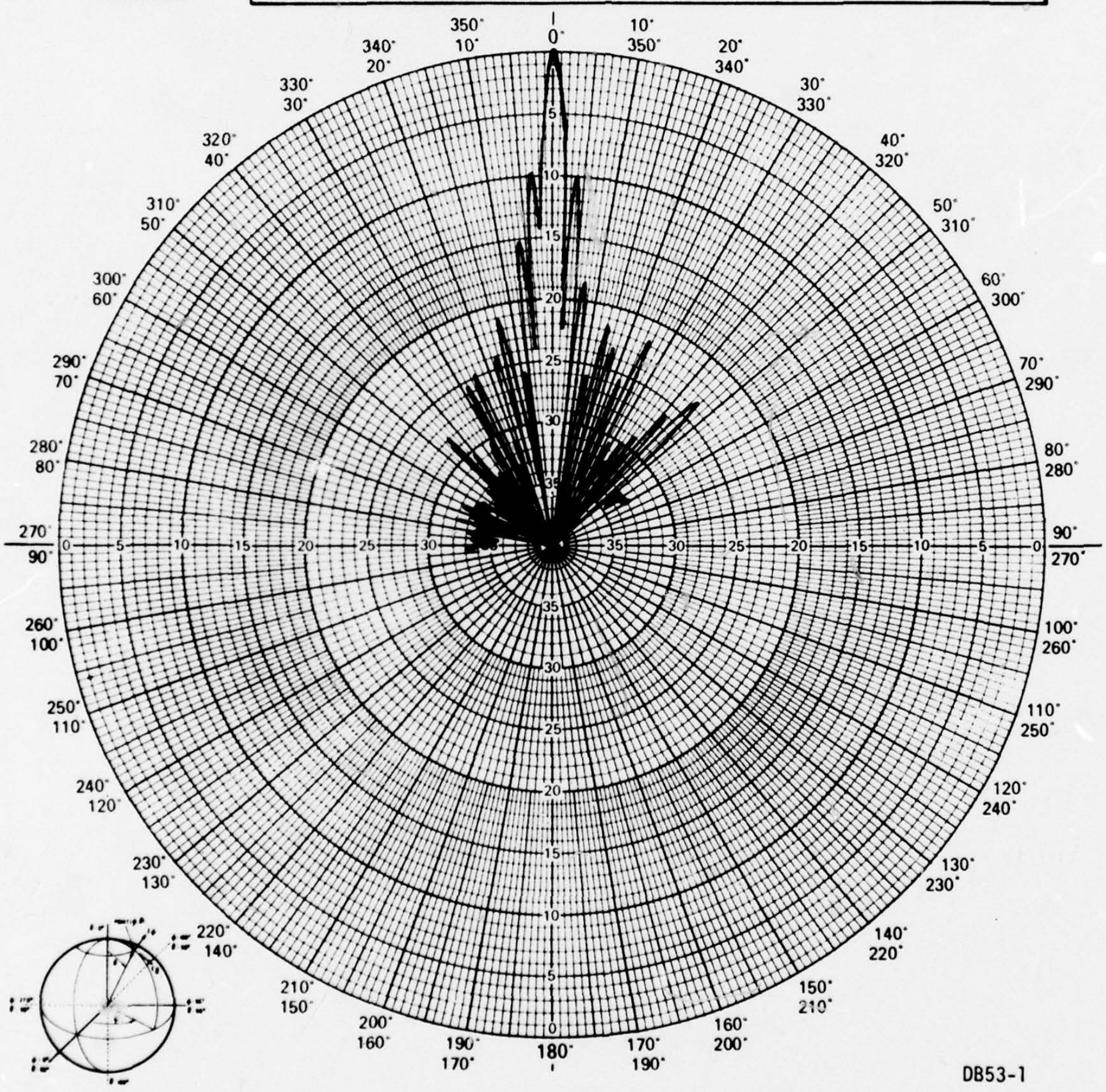

DB53-1
6/78

ORIENTATION

BALL AEROSPACE SYSTEMS DIVISION

REMARKS E-PLANE	POLARIZATION Eθ ☒ Eφ ☐ RC ☐ LC ☐ φ= θ=
	OPER. MW WITNESSED MW DATE 8/31/8

Figure 2-24 E-Plane Radiation Pattern (Serial #002, 38.7 GHz)

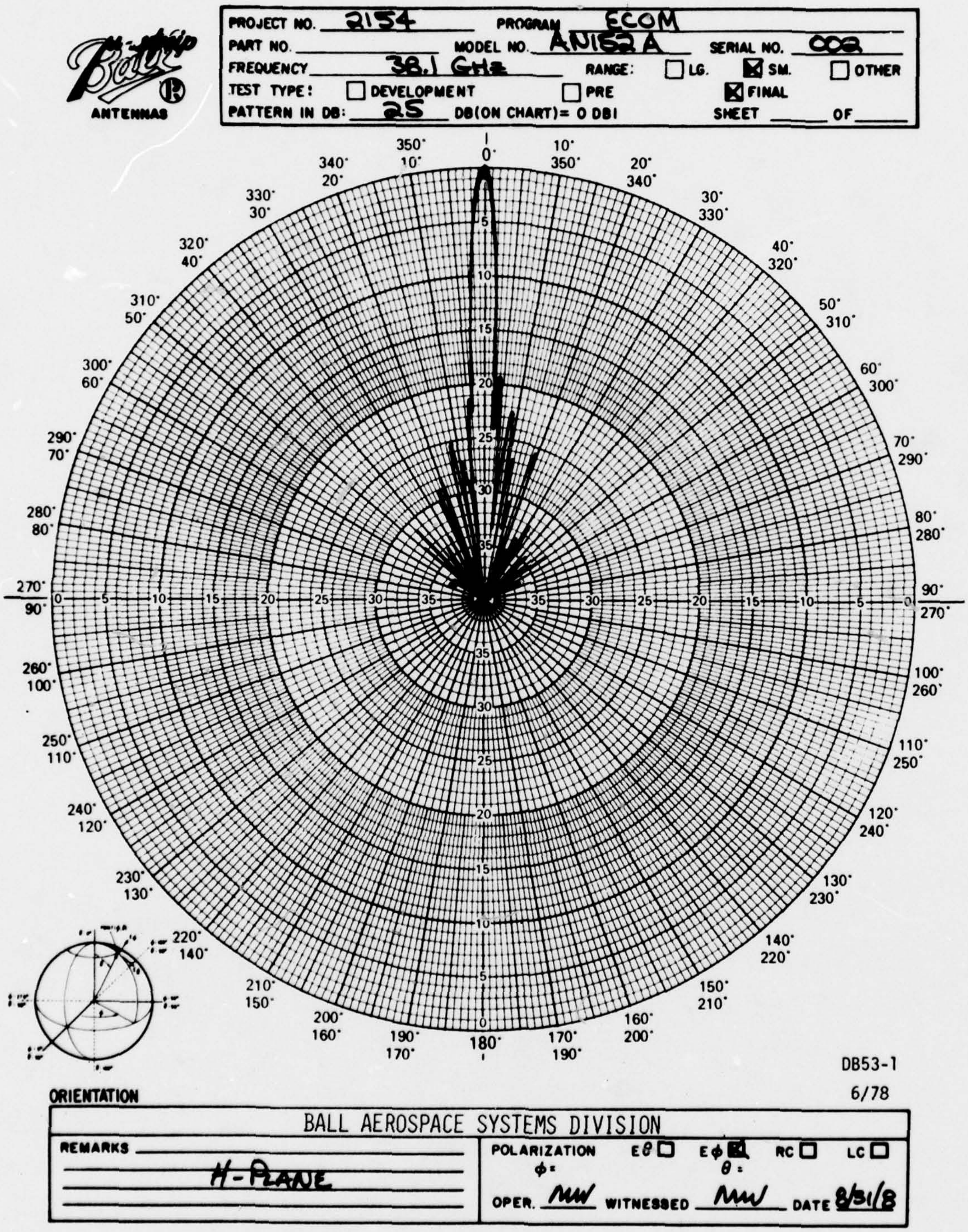

Figure 2-25 H-Plane Radiation Pattern (Serial #002, 38.1 GHz)

F78-16 Ball

Better ANTENNAS

PROJECT NO. 2154 PROGRAM ECOM
PART NO. ______ MODEL NO. AN152 A SERIAL NO. 002
FREQUENCY 38.4 GHz RANGE: ☐ LG. ☒ SM. ☐ OTHER
TEST TYPE: ☐ DEVELOPMENT ☐ PRE ☒ FINAL
PATTERN IN DB: 25 DB(ON CHART) = 0 DBI SHEET ______ OF ______

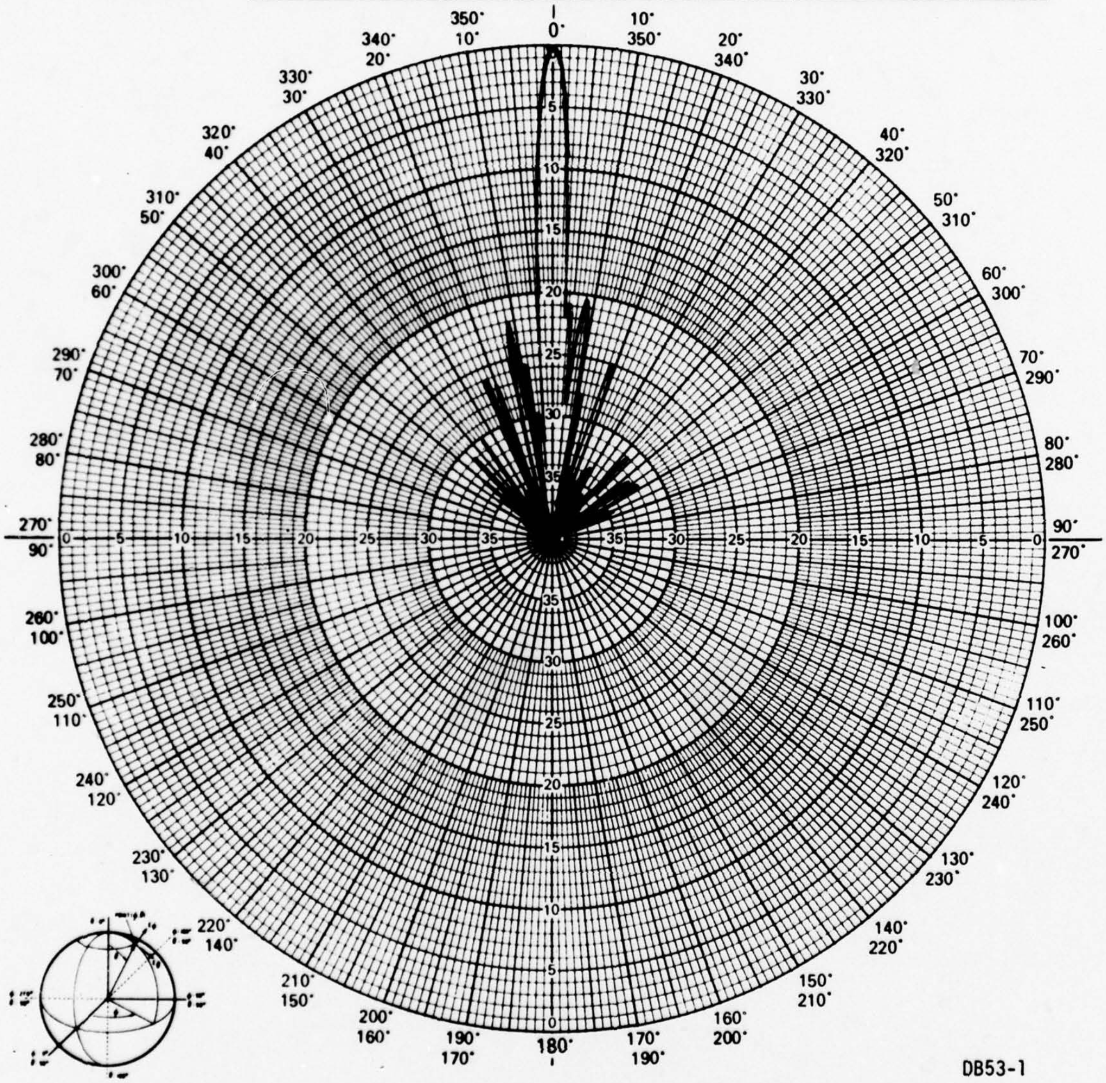

ORIENTATION

DB53-1
6/78

BALL AEROSPACE SYSTEMS DIVISION

REMARKS H-PLANE

POLARIZATION Eθ ☐ Eφ ☒ RC ☐ LC ☐
φ=
θ=
OPER. MW WITNESSED MW DATE 8/31/8

Figure 2-26 H-Plane Radiation Pattern (Serial #002, 38.4 GHz)

F78-16

Ball

Ball
ANTENNAS

PROJECT NO. 2154 PROGRAM ECOM
PART NO. ____ MODEL NO. AN152 A SERIAL NO. 002
FREQUENCY 38.7 GHz RANGE: ☐ LG. ☒ SM. ☐ OTHER
TEST TYPE: ☐ DEVELOPMENT ☐ PRE ☒ FINAL
PATTERN IN DB: 23 DB(ON CHART) = 0 DBI SHEET ____ OF ____

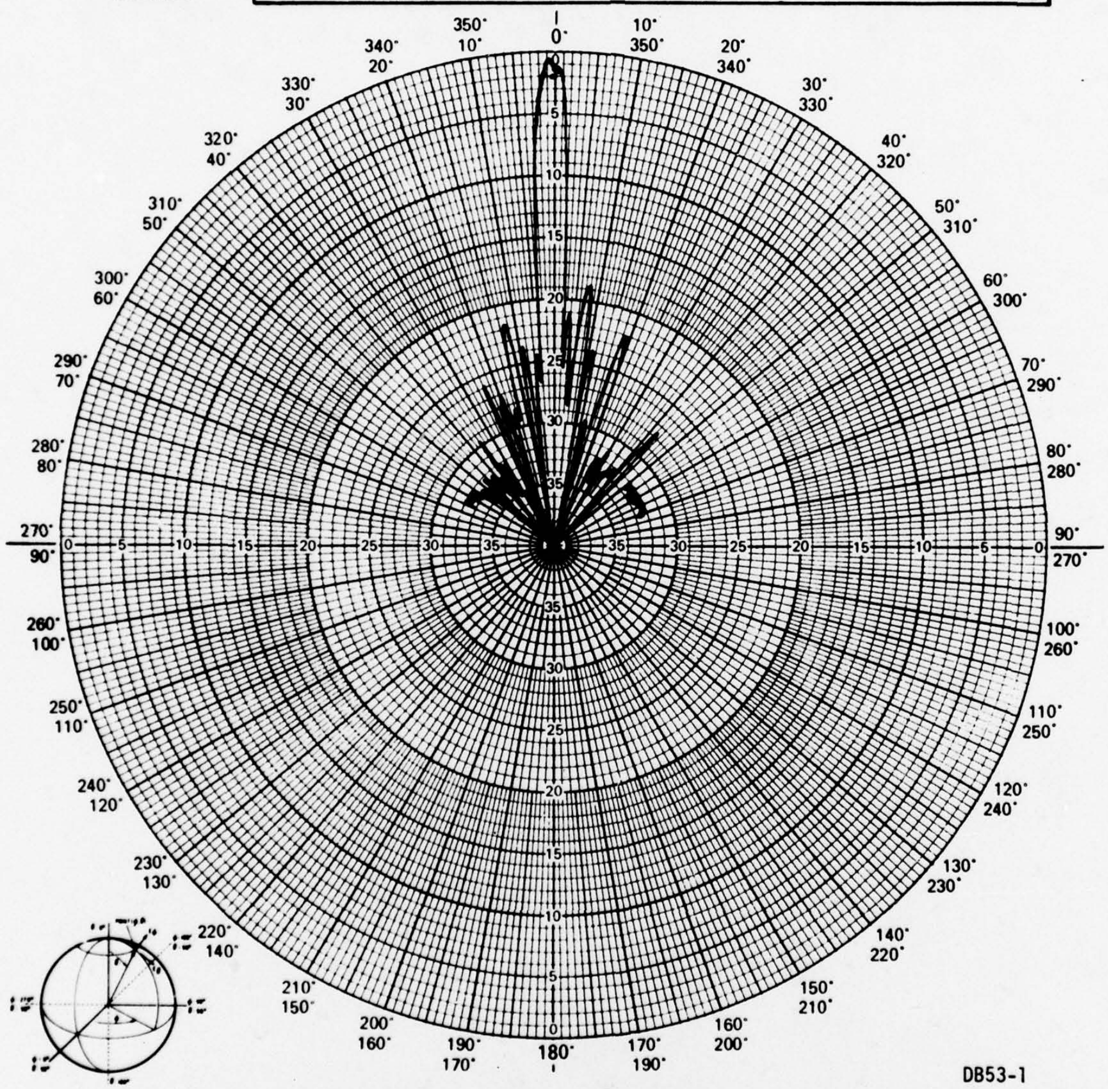

DB53-1
6/78

ORIENTATION

BALL AEROSPACE SYSTEMS DIVISION

REMARKS H-PLANE

POLARIZATION Eθ ☐ Eφ ☒ RC ☐ LC ☐
φ = θ =
OPER. MW WITNESSED MW DATE 8/31/8

Figure 2-27 H-Plane Radiation Pattern (Serial #002, 38.7 GHz)

Similar problems (and results) were encountered with the arrays fabricated for the front-end mixer integration portion of this study. A considerable amount of time was spent investigating the problem with the final conclusion being that the problem appeared to be caused by non-uniform substrate material. Variations in either substrate dielectric constant or thickness would cause an imbalance in the phase and amplitude relationship between the array elements. Some semblance of the proper conditions could be achieved by selected tuning (or detuning) of portions of the array; however, the power lost in these detuned areas is evident in the reduced gain level in S/N 002.

Following is a summary of array performance:

Theoretical Gain	37.7 dB
Measured Gain (S/N 001)	29.0 dB
Aperture Efficiency	0.9 dB
Mismatch Loss (VSWR = 2.0:1)	0.5 dB
Actual Gain	30.4 dB

Efficiency ≈ 37.7 dB - 30.4 dB ≈ 7.3 dB ≈ 19%

As previously mentioned, it is believed that a considerable portion of the 7.3 dB loss resulting in the low efficiency can be attributed to mismatches within the feed system. The antenna system loss budget shown in Table 2-2 gives an indication of the amount of power apparently lost in these mismatches.

Some of this 3.7 dB unexplained loss may be attributed to such things as non-uniform phase distribution on the radiating elements; however, it is believed that the majority of this number may be attributed to mismatch losses within the feed system caused by a non-uniform substrate.

2.5 32x32 ELEMENT ARRAY SUMMARY

Table 2-3 summarizes the performance parameters of S/N 001 and 002.

Table 2-2

LOSS BUDGET
S/N 001 (38.4 GHz)

Measured Gain	29.0 dB
Feedline Losses (≈0.6 dB/in* 3 in)	2.0 dB
Aperture Efficiency	0.9 dB
Waveguide Loss (≈15 dB/100 ft)	0.1 dB
Waveguide Power Divider Loss (2)	0.4 dB
Waveguide/Microstrip Transition Loss	0.3 dB
VSWR (2.0:1)	0.5 dB
Radiating Element Efficiency (≈80%)	0.8 dB
TOTAL	34.0 dB
Theoretical Gain	37.7 dB
Difference	3.7 dB

Table 2-3

SUMMARY OF ARRAY PERFORMANCE (AN152A)

Parameter		Design Goal	S/N 001	S/N 002
Frequency		38.4 GHz	38.4 GHz	38.4 GHz
VSWR		Less than 1.5:1	2.0:1	1.6:1
Bandwidth		200 MHz	>200 MHz (Pattern)	>200 MHz (Pattern)
Gain		$\geq$30 dB	29 dB	25 dB
Half-Power Beamwidth		$(2^{o}-4^{o})\times(2^{o}-4^{o})$	$\approx 2.4^{o} \times 2.3^{o}$	$2.5^{o} \times 2.5^{o}$
Side Lobe Level	E-Plane	-20 dB	-8/-11 dB	-10/-12 dB
	H-Plane	-20 dB	-13/-17 dB	<-20 dB
Efficiency		$\geq$50%	19%	7%
Size		5.5" x 5.5" x 0.25"	8.0" x 8.0" x 0.32"	8.0" x 8.0" x 0.32"

Section 3
RECEIVER FRONT-END CIRCUIT

3.1 SYSTEM DESIGN

The microstrip antenna receiver front-end circuitry is shown in block diagram form in Figure 3-1. This is a "typical" front-end design and was chosen for

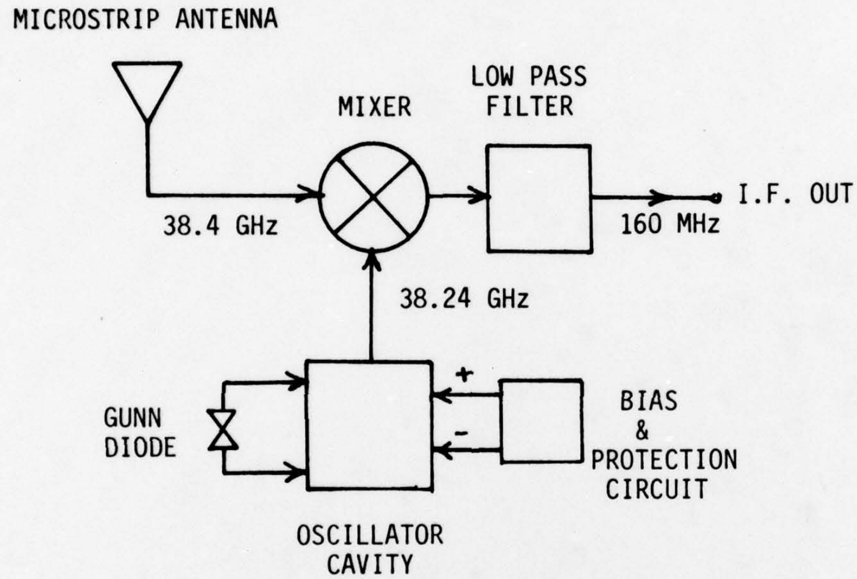

Figure 3-1 Antenna Receiver Front-End Block Diagram

its simplicity. The antenna itself forms the preselect filter and the signal is therefore band limited by the antenna and mixer combination only. The oscillator frequency is chosen to be 160 MHz below the antenna center frequency in order to produce an IF center frequency of 160 MHz. The output frequency is band limited only by the cabling and any subsequent circuits at the output of the mixer. The oscillator output is of such a level as to produce "saturation" of the Schottky-barrier mixer diodes. The frequency of operation for the oscillator is adjustable by means of a quarter-wave sliding short circuit and a mode suppressing screw. There is also some adjustment possible by varying the bias voltage to the oscillator. Figures 3-2 and 3-3 are front and rear views of the antenna-receiver system in its final form.

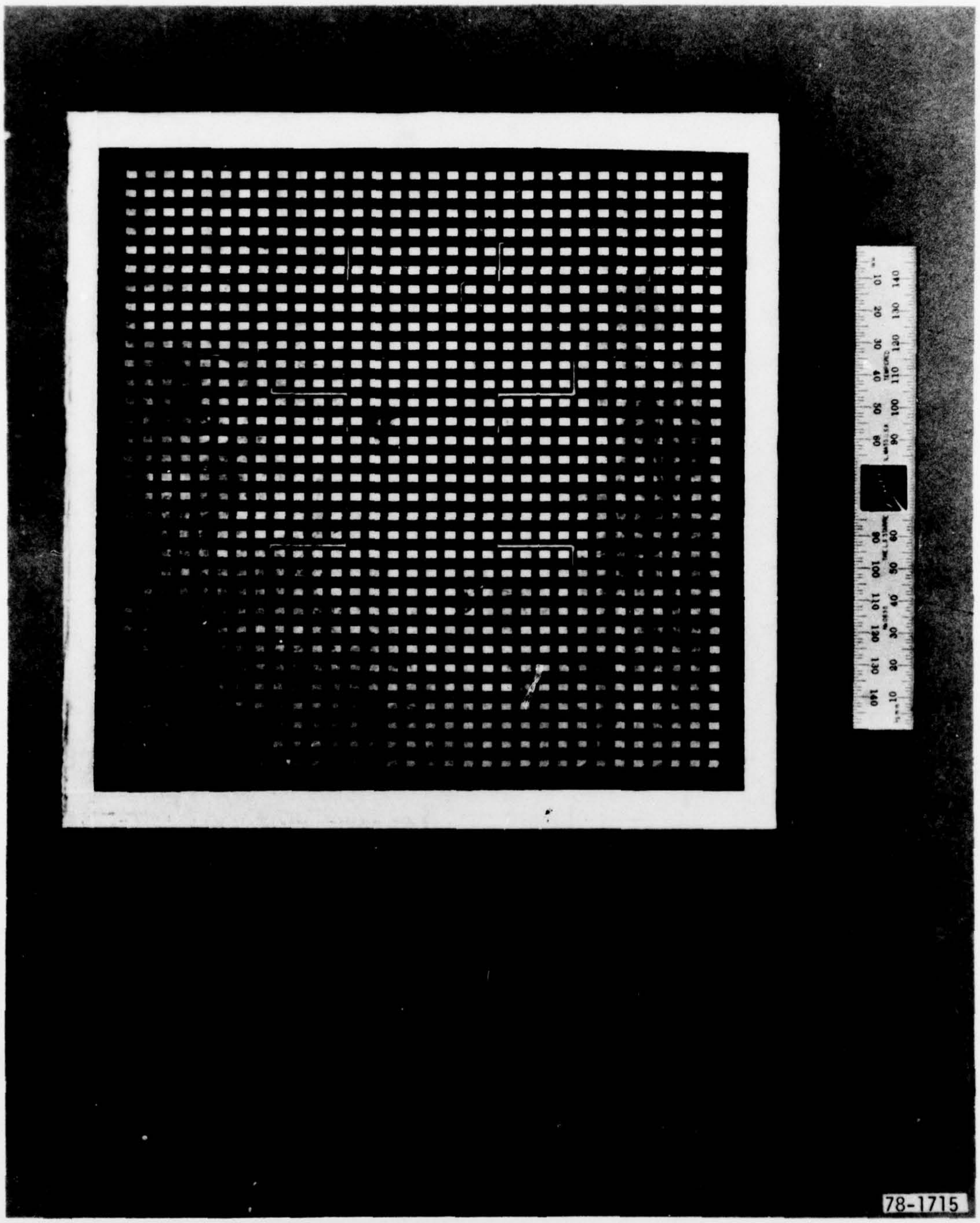

Figure 3-2 Antenna-Receiver System (Front View)

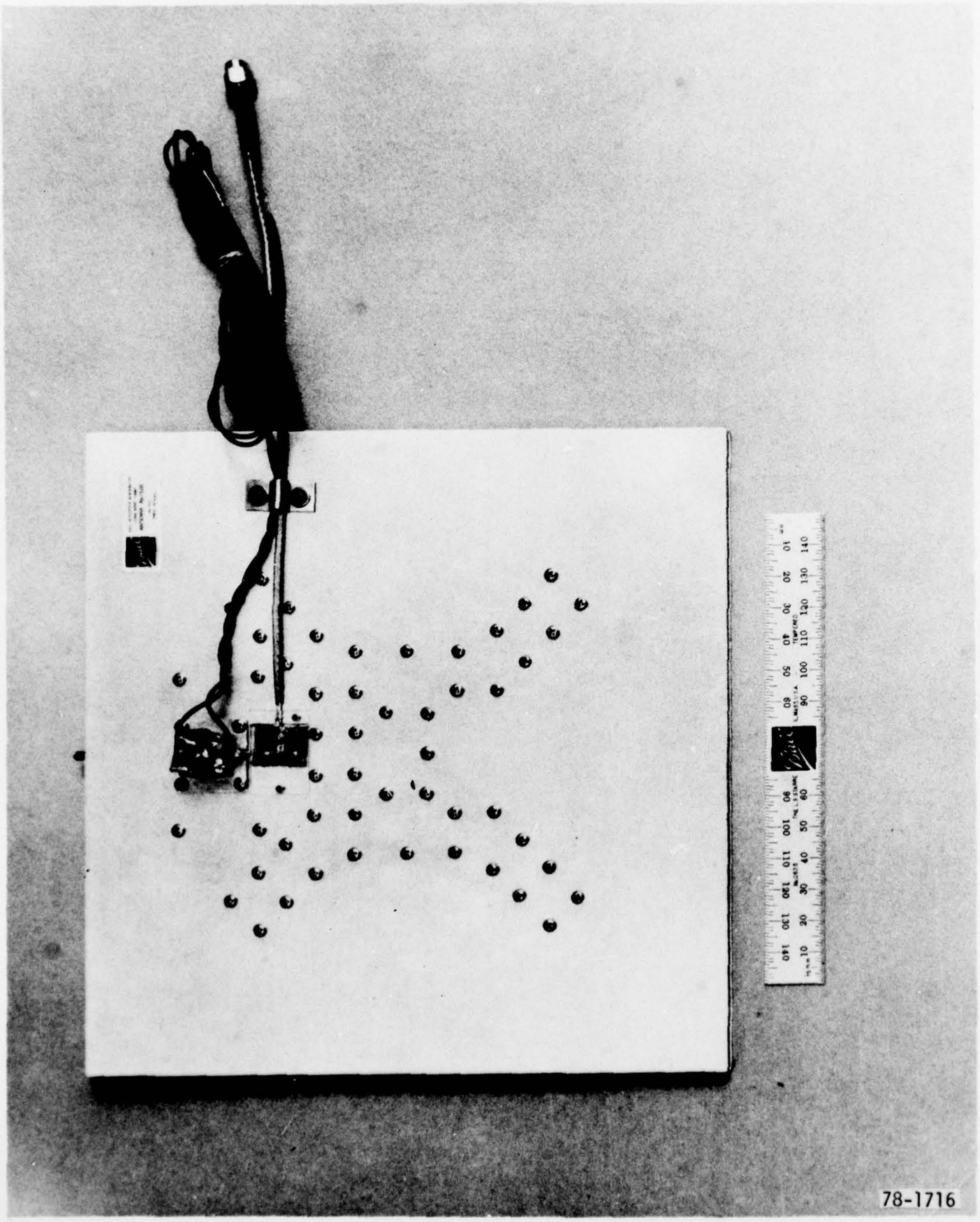

Figure 3-3 Antenna-Receiver System (Rear View)

3.2 GUNN EFFECT OSCILLATOR

The oscillator is a Gunn-effect diode oscillator. The diode is a Varian VSA9210S3 type in a stud-mount package. The diode is placed within a resonant cavity and voltage is applied. The present theory of operation is understood to be that a negative resistance is produced by a sudden change (decrease) in carrier mobility with increasing voltage (field strength). The frequency of oscillation is determined by the effects of the resonant cavity (its impedance) and the impedance of the diode itself.

The initial approach to the Gunn effect oscillator was a microstrip design. This type of circuit was used because it offered simplicity of design and ease of circuit change. The circuit is shown in diagram form in Figure 3-4.

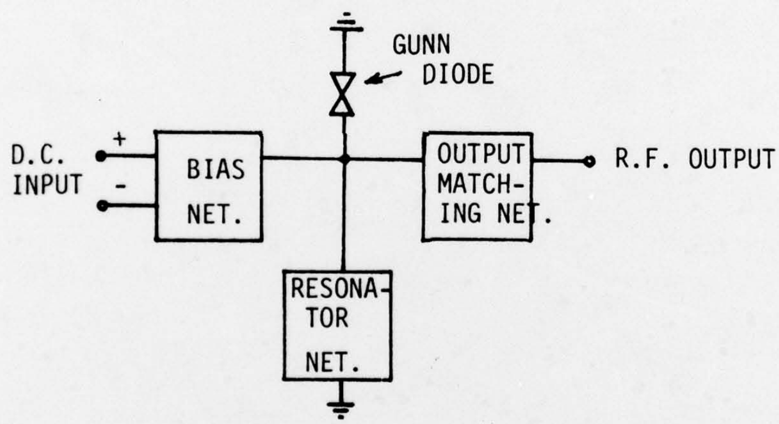

Figure 3-4 Gunn Oscillator Diagram

This is essentially the same as that used for the waveguide design. The circuit consisted of three basic parts: The biasing network, the output matching circuit and the resonator network.

The biasing network was dictated in part by the operating instructions from the manufacturer. This network consisted of a Zener diode for overvoltage

protection, a shunt capacitor for low frequency "spike" suppression and an R-C entwork for high frequency (>7 MHz) suppression. The output of this network was fed to the oscillator cavity (or resonant circuit) by way of a low-pass network (shown in Figure 3-5). This network is merely two pairs

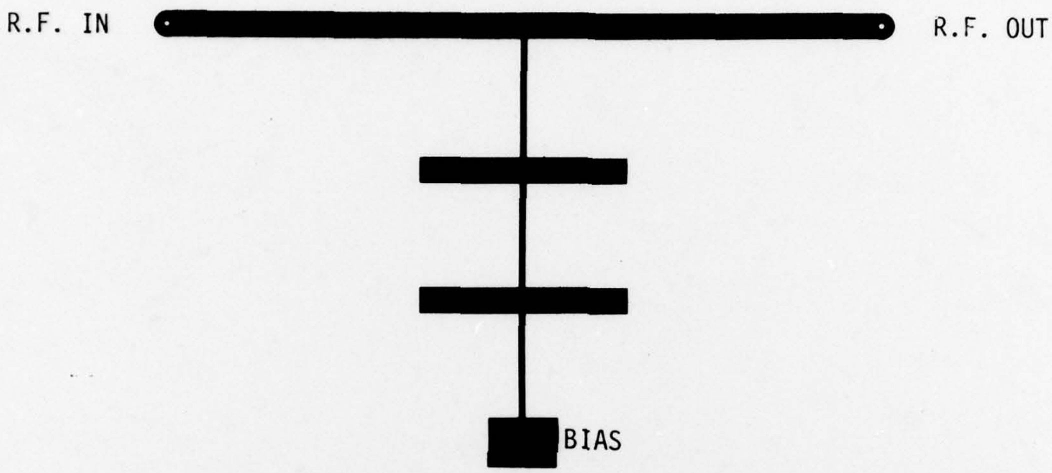

Figure 3-5 Microstrip Oscillator Low-Pass Filter Circuit

of open quarter-wavelength stubs, spaced one-quarter wavelength apart. Tests have shown this network to provide greater than 20 dB of suppression at 38 GHz. This network in turn is connected to the output line (50Ω) and is spaced more than a wavelenth away from the output of the oscillator and from the resonant circuit.

The Gunn diode and resonant circuit consist of a $\lambda/2$ wavelength resonator and a $\lambda/4$ matching transformer (see osc. layout, Figure 3-6). The resonator

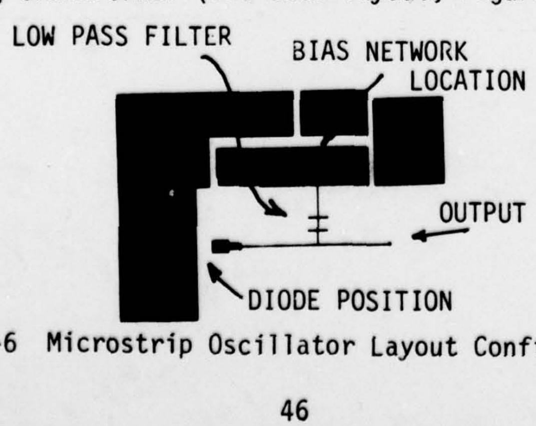

Figure 3-6 Microstrip Oscillator Layout Configuration

itself is less than $\lambda/2$ wavelengths wide and as such tends to suppress "moding" in the oscillator by disallowing the possibility of oscillations in the orthogonal direction of the microstrip patch. As is, the oscillator had a tendency to oscillate at a frequency near the required due to dual responses from the interaction of the matching transformer and the resonant circuit. Figure 3-7 is a computer printout based on the circuit model used for the microstrip case.

Frequency (GHz)		Impedance (Magnitude & Angle)		
P1	P2	Z1		
45.00	1.00	17.51	2.77	
44.00	1.00	18.31	-1.62	- 44.37 GHz
43.00	1.00	19.87	-6.01	
42.00	1.00	22.31	-10.33	
41.00	1.00	25.83	-14.40	
40.00	1.00	30.62	-17.83	
39.00	1.00	36.74	-19.95	
38.00	1.00	43.76	-19.80	
37.00	1.00	50.42	-16.61	
36.00	1.00	54.76	-10.67	
35.00	1.00	55.38	-3.84	
34.00	1.00	52.69	1.56	- 34.29 GHz
33.00	1.00	48.37	4.35	
32.00	1.00	43.97	4.69	
31.00	1.00	40.36	3.30	
30.00	1.00	37.85	0.90	

Figure 3-7 Computer Printout of Oscillator Output Impedance (Z1)

Wherever the output impedance (Z1) becomes real, a possibility of oscillation exists. The actual point of oscillation is greatly dependent on current as the diode negative resistance can vary over a fairly wide range. This circuit could be coarsely tuned by screwing the diode inward or outward from its mounting bracket, thus effectively increasing or decreasing the resonant cavity length. This method of tuning had the added feature of providing a small capacitance (a very short, open stub) in parallel with the diode.

The output circuit was to feed the mixer circuit directly such that the only waveguide probe was at the signal input to the mixer. Since the diode impedance was quite low (of the order of a few ohms), a matching transformer

(or transformers) was necessary. Thus, a one-quarter wavelength line was added between the diode resonator and the output 50Ω line. This line width (and thus its characteristic impedance) was determined experimentally and was of the order of 20 ohms.

The final configuration is shown in Figure 3-8. In this case, the diode has been placed in the center of the waveguide and is biased by means of a sliding "slug" type low-pass filter. The frequency of operation is determined by the radial line formed at the end of the "slug". This radial "cavity" is tuned by changing the separation between the radial cavity end and the bottom of the waveguide. This is accomplished by screwing the diode in or out and changing the fringing field capacitance at the edges of the radial line. This separation varies from a minimum of about 5 mils (0.005 in) to about 15 mils (0.015 in). This allows a tuning range of several GHz and provides a method of "rough" or coarse tuning. The diode may also be tuned by adjusting the DC voltage. This method provides a more fine tuning capability. Coarse tuning can also be accomplished by means of a "sliding" short at one end of the waveguide, but as this can also result in "mode-slipping", that is, the sudden discontinuous change in frequency with tuning, it is not recommended. The frequency and model stability can also be changed by means of the tuning screw located one wavelength away from the diode in the opposite direction from the sliding short. This screw is used mainly to reduce "mode-hopping" and really should not be used to change frequency. The theory behind this method is that the introduction of a capacitance about a wavelength away from the diode results in a frequency that produces a low impedance at that particular point in the waveguide. This theory assumes that standing waves exist in the guide and are of the TM_{10} mode. All other modes are assumed to produce high impedances at this spot and will therefore be cancelled by this effect.

3.3 SCHOTTKY DIODE MIXER

The mixer circuitry employed here consists of a 90^0 branch-line hybrid, two Schottky diodes and a low-pass summing network. Port 1 (Figure 3-9) is the signal input port (R.F.) and port 2 is the local oscillator (L.O.) input port.

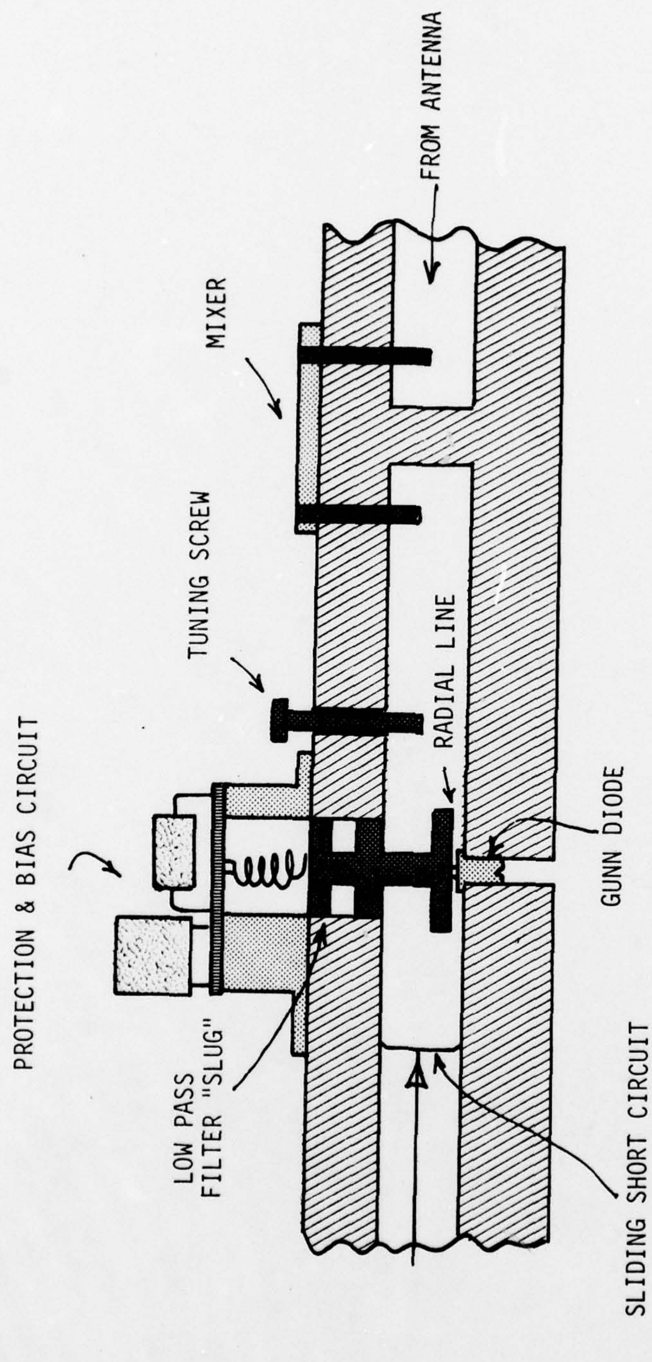

Figure 3-8 Oscillator Final Configuration

Figure 3-9 Layout for Schottky - Barrier Diode Mixer

This type of mixer configuration was chosen for its good VSWR, low conversion loss and good image rejection characteristics. Also because of its design, the image signal (2 L.O. - R.F.) will appear at the L.O. port. If this signal were to appear at the R.F. port, it is possible that reflection at some previous element (prior to mixer) would take place producing a second signal at the R.F. port and ultimately a signal or "image" at the I.F. frequency. A trade-off was made here and L.O./R.F. isolation was sacrificed to produce the best characteristics. This mixer type will commonly produce about 10 dB R.F. port to L.O. port isolation. Use of a 180^{0} mixer would have produced only about 10 dB more isolation but would have sacrificed the other parameters, i.e. VSWR, conversion loss and image rejection.

The lack of high (>30 dB) R.F. port to L.O. port isolation will result in re-transmission of a signal near the received signal (in frequency). This condition should not affect the incoming signal since it will be fairly well matched to the antenna and virtually no reflection will result.

Biasing of the mixer was considered for this development, but implementation of such techniques at Ka-band frequencies was thought to be too difficult for the return in better conversion loss. Also, biasing for low noise was not implemented for the same reasons.

The diodes are Alpha Industry Schottky barrier low noise beam-lead mixer diodes (DMK6606). Beam-lead diode packages were selected in order to reduce package parasitics and they lend themselves readily to MIC microstrip structures.

The summing and filtering port are of standard microstrip design. In this case, the summing function is merely an interconnect point for the mixed signal (difference) from either diode. Good, low VSWR design at this point is difficult as the diodes are operating in an extremely non-linear fashion and do not therefore have easily measurable reflection characteristics. However, an attempt to filter the local oscillator frequency component is made by introducing a open ended one-quarter wavelength stub at the summing position. This stub helps to reduce the L.O. signal at the I.F. port and provides a suitable return for R. F. energy from the local oscillator. A view of the bias circuit and mixer are shown in Figure 3-10.

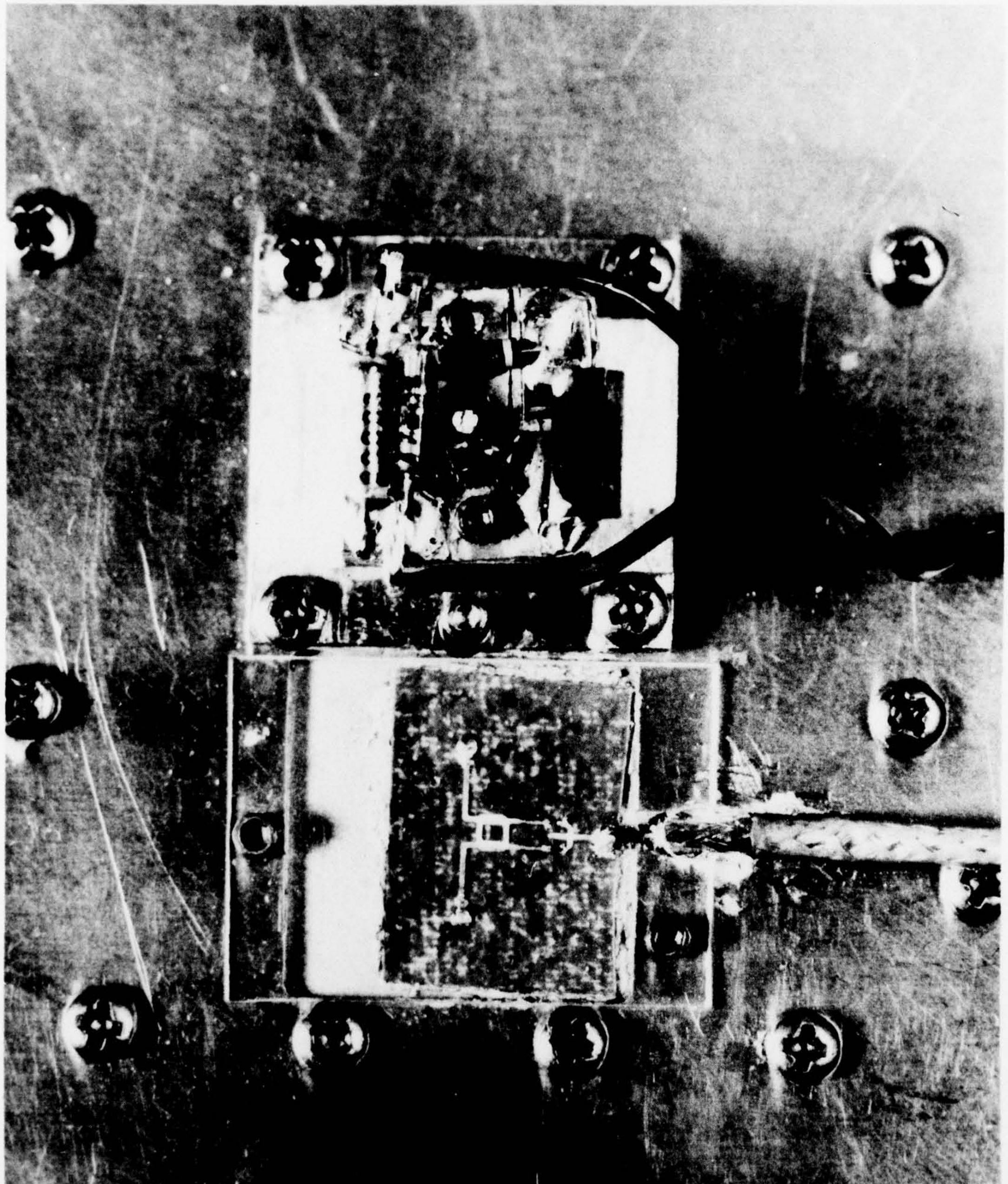

Figure 3-10 Protection-Bias Network and Mixer Photo

Section 4

CONCLUSIONS AND RECOMMENDATIONS

4.1 CONCLUSIONS

- 32 x 32 Element Array

The loss budget shown in Table 2-2 indicates approximately 3.7 dB of unexplained loss which has been attributed to mismatches within the feed system. Along with the corresponding gain loss, these mismatches also disrupt the inter-element phase/amplitude relationships, resulting in degraded pattern performance.

Since the scaled model of the 32x32 element array tested at 13.8 GHz performed essentially as predicted, it would appear safe to assume that the problem is not caused by a faulty design. (Even with an all microstrip feed network, the array produced $\approx$31 dB of gain with nearly -20 dB sidelobes in both the E and H-planes).

- Oscillator/Mixer

Although the mixer itself worked well, the oscillator produced considerable difficulty. Two problems were present from the beginning of operation of the oscillator and resulted in numerous diode failure and subsequently non-operative antenna-receiver systems. The first problem was that of bias circuit oscillation. It was found upon careful analysis of the bias circuit that an oscillation of the form found in relaxation-type oscillators could occur in the frequency range from 100 to 800 kHz. This problem was particularly difficult to spot as normal spectrum analysis did not provide enough resolution to show that oscillation was actually occurring. Secondly, these oscillations usually destroyed the diode in short order on an intermittent basis, so unless one was looking in the right place at the right time, everything appeared normal until sudden destruction occurred.

The second problem was that of multi-mode oscillations occurring in the wave guide itself. It was found that the oscillator would "jump" frequencies or oscillate at several frequencies at the same time depending on bias conditions and slider (sliding short circuit) position. In the final analysis the conclusion was that the oscillator was over-coupled to the mixer and was therefore very dependent on the impedance presented by the mixer. The mixer impedance, however, was very dependent on input level and therefore presented different impedances to the oscillator under different oscillator output levels. This interdependence along with the overcoupled condition made the oscillator more dependent upon the load presented to it than the cavity designed to determine the oscillator frequency. The results were then that the oscillator frequency was quite dependent upon its own output level. This problem did not occur during breadboard operation as some cable interconnection was required and the overcoupled condition did not exist.

The mixer performed well giving trouble only in fabrication stages and initial design stages. Conversion loss was a problem initially due to diode-coupler matching but was improved in subsequent design. The output impedance was not 50Ω as expected but was much lower and of the order of 10-15Ω. This results in an apparent conversion loss of near 16 dB but it is expected that with external matching the conversion loss can be improved to near 12 dB.

4.2 RECOMMENDATIONS

- 32 x 32 Element Array

Although some improvement in performance could probably be obtained by further refinements of the array feed system (waveguide and microstrip), it is felt that a detailed investigation of candidate substrate materials would result in the largest improvement in performance.

It may be necessary to employ substrates such as quartz to achieve the dielectric uniformity and low-loss tangent required for large arrays at millimeter frequencies.

- Oscillator/Mixer

The recommendation for the oscillator circuit would be a complete redesign based on a TEM structure. In this case, a coaxial type oscillator is proposed, using a positioned iris for coupling to waveguide or a simple resistive pad for isolation from the mixer. This circuit would have no tendency to oscillate at frequencies other than those described by the coaxial resonant circuit and would be more easily coupled to the mixer as both would be TEM mode circuits. This circuit also allows use of simpler biasing techniques and subsequent reduction in bias circuit induced oscillations.

The mixer performed well, although conversion loss was still not as good as hoped for. The solution here is merely better output matching and some slight changes in transmission line transformers for hybrid coupler to diode matching. Some work could also be done for noise figure improvement by possibly adding bias circuitry to the mixer.